Science Signaling
AAAS

www.sciencesignaling.org/cgi/content/full/8/377/ra49/DC1

Supplementary Materials for

The catalytic activity of the kinase ZAP-70 mediates basal signaling and negative feedback of the T cell receptor pathway

Hanna Sjölin-Goodfellow, Maria P. Frushicheva, Qinqin Ji, Debra A Cheng, Theresa A. Kadlecek, Aaron J. Cantor, John Kuriyan, Arup K. Chakraborty,* Arthur R. Salomon,* Arthur Weiss*

*Corresponding author. E-mail: as@brown.edu (A.R.S.); arupc@mit.edu (A.K.C.); aweiss@medicine.ucsf.edu (A.W.)

Published 19 May 2015, *Sci. Signal.* **8**, ra49 (2015)
DOI: 10.1126/scisignal.2005596

This PDF file includes:

Other Supplementary Material for this manuscript includes the following:
(available at www.sciencesignaling.org/cgi/content/full/8/377/ra49/DC1)

Table S1 (Microsoft Excel format). Complete list of sequence and phosphorylation site assignments of all identified phosphopeptides with corresponding SIC peak areas and statistics, protein association numbers, gene ontology, and KEGG functional annotation.
Table S2 (Microsoft Excel format). Complete list of phosphopeptides detected from every replicate and time point of TCR stimulation.

Experimental Procedures

Protein reduction, alkylation, digestion, and peptide immunoprecipitation

Cell lysates from ZAP-70^{AS} cells that were treated with inhibitor (heavy SILAC label) or were untreated (light SILAC label) were combined in equal proportions and reduced with 10 mM DTT for 20 min at 60°C, followed by alkylation with 100 mM iodoacetamide for 15 min at room temperature in the dark. Cell lysates were then diluted four-fold with 20 mM HEPES buffer (pH 8.0) and digested with sequencing-grade modified trypsin (Worthington) at a 1:1 (w/w) trypsin:protein ratio overnight at room temperature. Tryptic peptides were acidified to pH 2.0 by adding 1/20 volume of 20% trifluoroacetic acid (TFA) for a final concentration of 1% TFA, cleared at 1800*g* for 5 min at room temperature, and desalted with C18 Sep-Pak plus cartridges (Waters) as described previously (*34*), with the exception that TFA was used instead of acetic acid at the same required concentrations. Eluents containing peptides were lyophilized for 48 hours to dryness. Peptide immunoprecipitation was performed with p-Tyr-100 phosphotyrosine antibody beads (Cell Signaling Technology). Dry peptides from each time point were reconstituted in ice-cold immunoaffinity purification (IAP) buffer [5 mM MOPS (pH 7.2), 10 mM sodium phosphate, 50 mM NaCl] and further dissolved through gentle shaking for 30 min at room temperature and brief sonication in a sonicator water bath. Before peptide immunoprecipitation was performed, a 10-picomole fraction of synthetic phosphopeptide LIEDAEpYTAK was added to each time point sample as an exogenous quantitation standard. Peptide solutions were then cleared at 1800*g* for 5 min at room temperature, combined with p-Tyr-100 phosphotyrosine antibody beads, and incubated for 2 hours at 4°C. Beads were then washed three times with IAP buffer, twice with cold ddH_2O, and then were eluted with 0.15% TFA. Eluted peptides were desalted with C18 Zip Tip pipette tips (Millipore Corporation Billerica) as described previously (*79*).

Automated nano-LC/MS

LC/MS was performed as described previously (*34*). Tryptic peptides were analyzed by a fully automated phosphoproteomic technology platform (*80, 81*). Phosphopeptides were eluted into a Linear Trap Quadropole (LTQ)/Orbitrap Velos mass spectrometer (Thermo Fisher Scientific) through a PicoFrit analytical column (360-μm outer diameter, 75-μm inner diameter-fused silica with 15 cm of 3-μm Monitor C18 particles; New Objective) with a reversed phase gradient (0 to 70% 0.1 M acetic acid in acetonitrile in 60 min, with a 90-min total method duration). An electrospray voltage of 1.8 kV was applied using a split flow configuration, as described previously (*82*). Spectra were collected in positive ion mode and in cycles of one full MS scan in the Orbitrap (m/z: 300 to 1700), followed by data-dependent MS/MS scans in the LTQ (~ 0.3 s each), sequentially of the ten most abundant ions in each MS scan with charge state screening for the +1, +2, and +3 ions and a dynamic exclusion time of 30 s. The automatic gain control was 1,000,000 for the Orbitrap scan and 10,000 for the LTQ scans. The maximum ion time was 100 ms for the LTQ scan and 500 ms for the Orbitrap full scan. Orbitrap resolution was set at 60,000.

Data analysis

MS/MS spectra were searched against the nonredundant human UniProt complete proteome set database containing 72,078 forward and an equal number of reversed decoy protein entries using the Mascot algorithm provided with Matrix Science (*83*). Peak lists were generated with extract_msn.exe 07/12/07 using a mass range of 600 to 4500 m/z. The Mascot database search was performed with the following parameters: trypsin enzyme cleavage specificity, 2 possible

missed cleavages, 7 ppm mass tolerance for precursor ions, 0.5-Da mass tolerance for fragment ions. Search parameters specified a dynamic modification of phosphorylation (+79.9663 Da) on serine, threonine, and tyrosine residues, and methionine oxidation (+15.9949 Da), and a static modification of carbamidomethylation (+57.0215 Da) on cysteine. Search parameters also included a differential modification for arginine (+10.00827 Da) and lysine (+8.01420 Da) amino acids for the SILAC labeling. To provide high-confidence phosphopeptide sequence assignments, data were filtered for Mowse score (>20 for all charge states) for Mascot results. In addition, a logistic spectral score (*84*) filter was applied to achieve a final estimated decoy database estimated false discovery rate (FDR) of <1%. The FDR was estimated with the decoy database approach after final assembly of nonredundant data into heatmaps (*85*). To validate the position of the phosphorylation sites, the Ascore algorithm (*86*) was applied to all data, and the reported phosphorylation site position reflected the top Ascore prediction.

Quantitation of relative phosphopeptide abundance

Relative quantitation of phosphopeptide abundance was performed by calculation of select ion chromatogram (SIC) peak areas for heavy and light SILAC-labeled phosphopeptides. For label-free comparison of phosphopeptide abundance in ZAP-70AS cells that were not treated with inhibitor among different times of TCR stimulation, individual SIC peak areas were normalized to those of an exogeneously added standard phosphopeptide, LIEDAEpYTAK. The LIEDAEpYTAK phosphopeptide was added in the same amount to every LC/MS sample and accompanied cellular phosphopeptides through the peptide immunoprecipitation, desalt, and reversed-phase elution into the mass spectrometer. Peak areas were calculated by inspection of SICs with software programmed in Microsoft Visual Basic 6.0 based on Xcalibur Development kit 2.1 (Thermo Fisher Scientific). Quantitative data were calculated automatically for every assigned phosphopeptide with the ICIS algorithm available in the Xcalibur XDK. A minimum SIC peak area equivalent to the typical spectral noise level of 10000 was required of all data reported for label-free quantitation. A label-free data heatmap was generated for comparison of phosphopeptides through a time course of receptor stimulation as previously described (*34*). The magnitude of change of the heatmap color was calculated through the natural log of the ratio of the fold-change of each individual phosphopeptide peak area compared with the geometric mean for that phosphopeptide across all time points, as described previously (*34*). In the heatmap representation, the geometric mean of a given phosphopeptide across all time points was set to the color black. A blue color represented below average abundance, whereas yellow represented above average abundance for each unique phosphopeptide. Blanks in the heatmap indicated that a clearly defined SIC peak was not observed for that phosphopeptide in any of the replicate analyses for that time point. The heatmap colors were generated from the average of the LIEDAEpYTAK standard phosphopeptide normalized SICs in the five replicate experiments. The coefficient of variation (CV) was calculated for each heatmap square. Label-free *P* values were calculated from the replicate data for each time point compared to the time point with the minimum average peak area for that phosphopeptide. *Q* values for multiple hypothesis tests were also calculated for each time point based on the determined *P* values with the R package QVALUE as previously described (*43*, *44*). A white dot on a label free heatmap square indicated that a statistically significant difference (Q value < 5%) was detected for that phosphopeptide and timepoint relative to the timepoint with the minimal value. In the second type of heatmap, SILAC ratios corresponding to phosphopeptide abundance differences between ZAP-70AS cells that were treated with inhibitor or were left untreated across the time course of receptor

stimulation were represented (tables S1 and S2). For the SILAC heatmap, a black color represented a ratio of 1 between inhibitor-treated and control samples for the peak area of a given phosphopeptide at that time point. A red color represented less abundance, and green represented a higher abundance of the given phosphopeptide in ZAP-70^{AS} cells treated with inhibitor compared to ZAP-70^{AS} cells that were not treated with inhibitor. The magnitude of change of the heatmap color was calculated as described previously (*34*). Q values were also calculated based on replicate measurements for each phosphopeptide and time point (table S3). A white dot on a SILAC heatmap square indicated that a statistically significant change (Q value < 0.05) was observed between the replicate data from the samples of ZAP-70^{AS} cells treated with or without inhibitor for that time point and phosphopeptide.

Reproducibility of SILAC experimental data

Pairwise comparisons of phosphopeptide peak areas from individual samples were generated. To limit the effect of a few phosphopeptides with a large ratio, $\log_2$-transformed peak areas were used for these comparisons. There were 5 replicates per time point for SILAC light and heavy samples, and 160 nonredundant sample pairs could be constructed; fig. S1 shows a subset of these data for 20 plots corresponding to all 0-min sample pairs. The Pearson's correlation coefficient (*R)* indicated the degree of reproducibility. To provide a visualization of the similarity of individual samples for all 160 pairs, the dots from 80 pairwise comparison plots for heavy samples were shown in one plot (fig. S2A), and the Pearson's correlation coefficient was recalculated to indicate the reproducibility. The reproducibility of light samples was evaluated in the same way (fig. S2B).

Cell stimulation and lysate preparation for Western blotting validation of inhibitor specificity and SILAC data results

P116 cells reconstituted with WT or ZAP-70^{AS} were resuspended at 10^8 cells/ml in Dulbecco's PBS with Ca^{2+} and Mg^{2+} and allowed to rest at 37°C for 30 min. Ninety seconds before stimulation, the cells were treated with 10 μM HXJ42 or vehicle. OKT3 and OKT4 antibodies were added to the cells (to a final concentration of 0.25 μg/ml), and 30 s later, the antibodies were crosslinked with goat anti-mouse IgG at a final concentration of 22 μg/ml. At the indicated times, the cells were pelleted and lysed in ice-cold 1% NP-40 lysis buffer containing protease and phosphatase inhibitors. Lysates were centrifuged at 4°C for 15 min at 16000*g*. Lysates were then transferred into tubes containing an equal volume of 2× SDS sample buffer containing 2-mercaptoethanol. Lysates were resolved by SDS-PAGE, transferred to Immobilon membranes, and then Western blotting analysis was performed. Data are representative of at least three independent experiments (fig. S3).

Antibodies

The following antibodies were used: OKT3, OKT4 (eBiosciences); anti-LAT-pY132 (Invitrogen/BIOSOURCE); anti-ZAP70-pY319, anti-ZAP-70-pY493, anti-p44/42 MAPK pThr202/Tyr204 (Cell Signalling); anti-Lck (1F6 from J. B. Bolen); anti-pY (4G10; Upstate Biotechnology); nti-LAT (Abcam); anti-ERK1/2, anti-SLP-76 (Santa Cruz Biotechnology Inc.); anti-CD3ζ-pY142 (BD Pharmingen); anti-pY128-SLP-76 (BD Biosciences); horseradish peroxidase (HRP)-conjugated goat anti-rabbit IgG (H+L) and goat anti- -mouse IgG (H+L)-HRP (Southern Biotech). The following antibodies have been described previously: 2F3.2 (anti-ZAP-70) and 6B10.2 (anti-CD3ζ).

Measurement of the binding affinities of Lck-SH2 for singly phosphorylated ITAMs

The Lck SH2 domain (amino acid residues 126 to 223) was expressed in *E. coli* with an N-terminal hexahistidine and protein G tag. It was purified with a nickel affinity capture step, followed by tag removal using TEV protease, a subtractive nickel affinity step, and size-exclusion chromatography. The concentration of the Lck SH2 domain was determined spectrophotometrically by the method of Edelhoch (*87*), with a calculated extinction coefficient of 9530 M^{-1} cm^{-1} at a wavelength of 280 nm. The singly phosphorylated ITAM peptides, corresponding to amino acid residues 69 to 87 of human TCR ζ, were synthesized by ELIM Biopharmeceuticals. Peptide concentrations were determined spectrophotometrically at a wavelength of 205 nm with an extinction coefficient of 66,500 M^{-1} cm^{-1}, as calculated by the method of Anthis and Clore (*88*). Isothermal titration calorimetry (ITC) was performed with an auto-ITC_{200} instrument (GE) at 25°C. Before the experiments, the protein and peptides were dialyzed for ≥24 hours against binding buffer containing 25 mM hepes (pH 7.5), 150 mM NaCl, 1 mM TCEP, with two changes of buffer. The Lck SH2 domain was used as the syringe titrant, and the peptide was used as the cell reactant. After an initial injection of 0.5 µl, 19 injections of 2 µl of the Lck SH2 domain into the peptide were recorded. Fitting was performed with the Origin software provided by the instrument manufacturer with a one-set-of-sites model after subtracting a constant value of from the integrated heats to correct for the heat of dilution. The reported binding parameters are from a single experiment that is representative of two independent experiments (fig. S4 and table S4).

Computational Modeling

The plasma membrane environment affects the kinetics of Lck

The experimental ZAP-70 null / ZAP-70 reconstituted SILAC ratio shows an asymmetry in the phosphorylation of the N- and C-terminal tyrosine residues in each ζ-chain ITAM (Fig. 5A). To reproduce this asymmetry, we used previous observations found in B cells (*89*). Specifically, the Src family kinase, Lyn, binds through its SH2 domain to singly phosphorylated ITAMs. Once bound, Lyn increases its catalytic activity and rapidly phosphorylates the neighboring site in the ITAM. We applied these observations to our calculations of T cells with the Src family kinase, Lck. The calculated SILAC ratios using these effects (the "ITAM and Lck" model, Fig. 5A) require that the Lck SH2 domain binds to the singly phosphorylated ITAMs with high affinity (comparable to the binding affinity of ZAP-70 for doubly phosphorylated ITAMs). Once bound, Lck rapidly phosphorylates the neighboring terminal tyrosine residues within each ζ-chain ITAM (with faster kinetics than those of the initial ITAM phosphorylation), generating the doubly phosphorylated ITAMs. These faster kinetic effects may emerge from the effect of the plasma membrane environment, because Lck is located, by virtue of its myristoylation and palmitoylation, in the plasma membrane, whereas ZAP-70 has no lipid modification and is found in the cytoplasm. The plasma membrane environment results in increased protein concentrations and correlations in two dimensions that result in enhanced rebinding events. This may result in a higher fraction of bound enzyme-substrate pairs (*72, 73*). To test this assumption, we roughly estimated the number of the rebinding events of Lck-SH2 to the singly phosphorylated ITAMs.

The number of enzyme-substrate rebinding events was calculated with Bell's model (*90*) for the membrane [two-dimensional (2D) case] and the cytoplasm (3D case) environments. The total dwell time t_a over the duration of all rebinding events is (*91*):

$$t_a = t_{1/2} + \frac{1}{K_D} \cdot \left[\frac{\ln(2)}{k_{on}^*} \right] \quad \text{(S1)}$$

$$k_{on}^* = 2\pi(D_E + D_s) \quad \text{(S2)}$$

where k_{on}^* is a threshold k_{on} above which rebindings are relevant, and D_E and D_s are the diffusion constants of the enzyme and substrate, respectively. In general, whenever k_{on} exceeds this threshold, at least one rebinding is expected to occur. In the membrane environment, the threshold k_{on}^* value equals 60,000 μm^2/s, whereas in the cytoplasm it is $5 \cdot 10^8$ μm^2/s [taken from (*90*, *91*)]. The half-time $t_{1/2}$ accounts for the duration of the first binding event, whereas the second term of equation S1 accounts for any subsequent rebinding events. Because the duration of every individual binding events lasts, on average, for as long as any other, the expected number of rebinding events between enzyme and substrate is (*91*):

$$\bar{N} = \frac{t_a}{t_{1/2}} - 1 = \frac{k_{on}}{k_{on}^*} \quad \text{(S3)}$$

Depending on the k_{on} and k_{on}^* values (here, we associate them with the substrate binding affinity K_D and the diffusion coefficient, respectively), the system has qualitatively different behavior (shown in fig. S5). When k_{on} rates are high (high binding affinity), many rebinding events occur between the enzyme and substrate, reaching quasi-equilibrium before they diffuse away from each other. However, when k_{on} rates are low (low binding affinity), the rebinding events occur very rarely. Additionally, upon moving from the cytoplasm to the membrane environment [by decreasing the diffusion coefficient (or the threshold value k_{on}^*)], the number of rebinding events increases.

Furthermore, fig. S5 also provides a good correlation with the experimentally measured binding affinities of the Lck SH2 domain to singly phosphorylated ITAMs and of ZAP-70 to doubly phosphorylated ITAMs (*66*). The top left corner of fig. S5 represents a low number of rebindings of ZAP-70 to the singly phosphorylated ITAMs, which is consistent with its low binding affinity [5 μM (*66*)]. ZAP-70 binds strongly to doubly phosphorylated ITAMs [k_D ~5 nM (*65*, *66*)]. Therefore, the number of the rebinding events increases (as illustrated in the top right corner of fig. S5). The measured binding affinity of the Lck SH2 domain to the singly phosphorylated ITAM in solution is low [1 μM (*66*)], and thus one would expect a low number of rebinding events; however, we assumed that Lck is in the membrane environment, and therefore the number of rebindings is high (shown at the bottom right corner of fig. S5). Therefore, the binding affinity of the Lck SH2 domain for the singly phosphorylated ITAM could potentially be comparable to that of ZAP-70 for doubly phosphorylated ITAMs. However, this assumption requires further experimental measurements of the Lck-SH2 binding affinity for singly phosphorylated ITAMs in the membrane environment.

Estimate of the high effective concentration of Lck

To explain the ITAM asymmetry of ZAP-70 null cells (Fig. 5A) through computational modeling, we found that the Lck-SH2 has to bind strongly to singly phosphorylated ITAMs. Once bound, Lck then rapidly phosphorylates the neighboring terminal tyrosine residues within each ζ-chain ITAM with faster kinetics than that of the initial ITAM phosphorylation event. This is because the strongly bound Lck has a higher effective concentration for the phosphorylation of the neighboring tyrosine. Namely, once Lck binds to singly phosphorylated ITAMs, its high effective concentration promotes the faster phosphorylation of the adjacent site in the ITAM.

Using Michaelis-Menten kinetics, we estimated the effective concentration of Lck that is localized to the singly and doubly phosphorylated ITAMs and compared it to the amount of ZAP-70 that was bound to the doubly phosphorylated ITAMs.

$$E + S \leftrightarrow E{:}S \tag{S4}$$

$$K_D = [E][S] / [ES] \tag{S5}$$

$$[E] + [ES] = [E]_0 \tag{S6}$$

where E is enzyme, S is substrate, E:S is the enzyme-substrate complex, K_D is a dissociation constant, [E] is the concentration of free enzyme, [ES] is the concentration of bound enzyme, and $[E]_0$ is total enzyme concentration. Lck and ZAP-70 are enzymes and the singly and doubly phosphorylated ITAMs are substrates.

Substituting equation S6 into equation S5, we obtained:

$$K_D = ([E]_0 - [ES])\,[S] / [ES] = ([E]_0 / [ES] - 1)\,[S] \tag{S7}$$

If we assume that $K_D >> [S]$, leading to

$$K_D \approx [E]_0 / [ES] \tag{S8}$$

then the concentration of bound enzyme is

$$[ES] = [E]_0 / K_D \tag{S9}$$

Using equation S9 and experimentally measured binding affinities, we calculated the effective concentrations of Lck and ZAP-70 bound to the singly and doubly phosphorylated ITAMs. First, we calculated the concentration of Lck bound to the singly phosphorylated ITAMs:

$$Lck(A,SH2) + ITAM(N_p,C_0) \leftrightarrow Lck(A,SH2){:}ITAM(N_p,C_0) \tag{S10}$$

$$K_{D1}^{Lck} = [Lck(A,SH2)][ITAM(N_p,C_0)] / [Lck(A,SH2):ITAM(N_p,C_0)] \quad (S11)$$

Substituting equation S9 into equation S11, we obtained:

$$[Lck(A,SH2):ITAM(N_p,C_0)] = [Lck(A,SH2)][ITAM(N_p,C_0)] / K_{D1}^{Lck} \approx [Lck(A)]_0 / K_{D1}^{Lck} \quad (S12)$$

If the total concentration of Lck $[Lck(A)]_0$ = 1.67 μM (estimated from our calculations) and $K_{D1}^{Lck,exp}$ = 5 μM (*66*), then the concentration of Lck bound to the singly phosphorylated ITAMs $[Lck(A,SH2):ITAM(N_p,C_0)]$ = 0.334 μM. Once Lck binds through its noncatalytic SH2 domain to the singly phosphorylated ITAMs, it rapidly binds with its catalytic domain to the neighboring terminal tyrosine residues within each ITAM and promotes the subsequent phosphorylation events:

$$Lck(A,SH2):ITAM(N_p,C_0) \leftrightarrow Lck(A,SH2):ITAM(N_p,C_0):Csite \quad (S13)$$

$$K_{D2}^{Lck} = [Lck(A,SH2):ITAM(N_p,C_0)]/ [Lck(A,SH2):ITAM(N_p,C_0):Csite] \quad (S14)$$

Therefore, the amount of Lck bound to ITAMs is given by:

$$[Lck(A,SH2):ITAM(N_p,C_0):Csite] = [Lck(A,SH2)][ITAM(N_p,C_0)] / K_{D1}^{Lck} \cdot K_{D2}^{Lck} \quad (S15)$$

Substituting equation S9 into equation S15, we obtained:

$$[Lck(A,SH2):ITAM(N_p,C_0):Csite] \approx [Lck(A)]_0 / K_{D1}^{Lck} \cdot K_{D2}^{Lck} \quad (S16)$$

If K_{D2}^{Lck} = 5 μM (estimated from the fact that ZAP-70 binds more strongly to the doubly phosphorylated ITAMs than does Lck ($K_D^{ZAP-70,exp} > K_{D1}^{Lck,exp} \cdot K_{D2}^{Lck}$)), then the concentration of bound Lck to ITAMs $[Lck(A,SH2):ITAM(N_p,C_0):Csite]$ = 66,800 μM.

Next, we calculated the amount of ZAP-70 bound to the doubly phosphorylated ITAMs.

$$ZAP\text{-}70 + ITAM(N_p,C_p) \leftrightarrow ZAP\text{-}70:ITAM(N_p,C_p) \quad (S17)$$

$$K_D^{ZAP-70} = [ZAP\text{-}70][ITAM(N_p,C_p)] / [ZAP\text{-}70:ITAM(N_p,C_p)] \quad (S18)$$

Substituting equation S9 into equation S18, we obtained:

$$[ZAP\text{-}70:ITAM(N_p,C_p)] = [ZAP\text{-}70][ITAM(N_p,C_p)] / K_D^{ZAP-70} \approx [ZAP\text{-}70]_0 / K_D^{ZAP-70}$$

If the total concentration of ZAP-70 $[ZAP\text{-}70]_0$ = 0.83 μM (estimated from our calculations) and $K_D^{ZAP\text{-}70,exp}$ = 5 nM (*66*), then the concentration of ZAP-70 bound to the doubly phosphorylated ITAMs [ZAP-70:ITAM(N_p,C_p)] = 166 μM.

These estimates provide support for the increased kinetic effects considered in our computational model. The amount of ZAP-70 bound to the doubly phosphorylated ITAMs is greater than the amount of Lck bound to the singly phosphorylated ITAMs, which is consistent with the experimentally measured binding affinities of Lck and ZAP-70 (*66*). In addition, our estimates showed that once Lck binds with its SH2 domain to the singly phosphorylated ITAMs, its effective concentration increases and further promotes subsequent phosphorylation events. This is similar to observations of B cells (*89*).

Additional computational model: Including ZAP-70 allosteric function

A study of ITAM-ζ1 peptide binding affinities to ZAP-70 (*65*) suggests another mode of regulation of ZAP-70. Deindl *et al.* (*65*) showed that WT ZAP-70 in its open conformation binds to the ITAM-ζ1 peptide with high affinity (K_D = 76.7 nM). The mutations Y315F and Y319F in the SH2-linker domain of ZAP-70, which stabilize its auto-inhibited conformation, slightly reduced the binding affinity of the mutant ZAP-70 for the ITAM peptide (K_D = 96.1 nM). This difference in the binding affinities suggests the possibility that the allosteric regulation of ZAP-70 may affect its ability to bind to ITAMs. Therefore, an inhibitor in the ZAP-70^{AS}+Inhibitor cells might influence ZAP-70 conformation along with its kinase activity. To explore the consequences of this allosteric regulation of ZAP-70, we incorporated this effect into our model (fig. S6).

The model for the ZAP-70-reconstituted cells and the ZAP-70^{AS} cells includes the sequential phosphorylation of ITAMs by active Lck (Fig. 4A) and the binding of auto-inhibited ZAP-70 to singly and doubly phosphorylated ITAMs (Fig. 4B). Here, the autoinhibited ZAP-70 bound to the doubly phosphorylated ITAMs (fig. S6) with slightly reduced affinity (K_D = 96.1 nM). Next, active Lck phosphorylates tyrosines Y315 and Y319 in the ZAP-70 SH2-linker domain, leading to a conformational change in ZAP-70 (to open ZAP-70), and therefore to an increase in the binding affinity of ZAP-70 to the doubly phosphorylated ITAMs (K_D = 76.7 nM). After this, active Lck phosphorylates the catalytic domain activation loop of ZAP-70 to generate active ZAP-70. In our model for ZAP-70^{AS}+Inhibitor cells, the inhibitor keeps ZAP-70 in its open conformation, thus increasing its binding affinity for ITAMs (K_D = 76.7 nM). It also excludes the last ZAP-70 phosphorylation step, which converts ZAP-70 from the basal to the active state (because the inhibitor blocks the kinase activity of ZAP-70).

Upon incorporating the allosteric regulation of ZAP-70, the calculated ZAP-70 null / ZAP-70 reconstituted SILAC ratio decreased for the N- and C-terminal tyrosines within each ITAM (fig. S6). However, the calculated ZAP-70^{AS}+Inhibitor / ZAP-70^{AS} SILAC ratio increased somewhat for both the N- and C-terminal tyrosines in the ζ-chain ITAMs (fig. S6). The calculated SILAC ratio of the ZAP-70 null / ZAP-70-reconstituted cells decreased because of the protective function of ZAP-70. Thus, including the allosteric regulation of ZAP-70 can explain the experimental data on the ZAP-70^{AS}+Inhibitor / ZAP-70^{AS} SILAC ratio. However, this mechanism can never allow an increase in the SILAC ratio of the ZAP-70 null / ZAP-70-reconstituted cells, because this enables only the protective function of ZAP-70, which will

always increase ITAM phosphorylation. Our observation that the SILAC ratio of the ZAP-70 null / ZAP-70-reconstituted cells increased for the C-terminal tyrosines led us to not explore this effect any further.

Kinetic parameters estimates and sensitivity analysis

The kinetic parameters used in our computer simulations are listed in tables S5 to S7. The rate constants for several reactions were taken from the corresponding in vitro experiments or were estimated from the relevant biological experiments. However, our calculations used a few unknown kinetic parameters, for which we performed an extensive sensitivity analysis to test the robustness of our main results to a wide range of parameter variations. The results of parameter sensitivity analysis are listed in tables S8 to S12 and are illustrated in figs. S7 to S10. We varied each reaction rate and concentration parameter independently (while keeping other parameters fixed) by a large discrete change, with decreasing and increasing the parameters by several factors for concentrations and rate constants from their base value, and calculated the response from our proposed model. Many kinetic parameters variations showed no qualitative changes in our main results, revealing the robustness of our proposed model. We also identified several sensitive parameters whose variations produced some qualitative changes in our results. However, the variations of some rate constants introduced pathological biological situations, and thus were excluded.

Concentration estimates and their sensitivity analysis

Here, we used estimates of concentrations in our calculations and subjected them to sensitivity analysis by varying each concentration by several factors from its base value. Variations in either direction in the concentrations of Lck, ITAM, ZAP-70, and all phosphatases in either direction had no qualitative effects on our results (tables S8 and S11).

Rate constant estimates and their sensitivity analysis

The rate constants for several reactions were estimated from the relevant biological experiments. The unknown rate constants were varied by several factors from their base values. Variations in many rate constants in either direction resulted in no qualitative change in our results (tables S9, S10, and S12). Variations of several rate constants showed sensitive responses in our simulations (described in the section entitled "Sensitive kinetic parameters"). However, variations of some rate constants introduced pathological biological situations and were excluded from the valid parameter range. For example, ZAP-70 protects singly phosphorylated ITAMs from the actions of phosphatases at high k_{on} (ZAP-70 binding to singly phosphorylated ITAMs), and competes with the binding of the Lck SH2 domain to singly phosphorylated ITAMs or with the binding of ZAP-70 to the doubly phosphorylated ITAMs (fig. S8, C and D; fig. S10, A and B; and tables S9, S10, and S12). Another pathology was observed for high k_{off} values for all phosphatases, because the phosphatases dissociate before causing dephosphorylation (tables S9, S10, and S12).

Sensitive kinetic parameters

Several kinetic parameters (mainly unknown rate constants) showed sensitive responses in our simulations because of many uncertainties in the parameter values. The first set of sensitive parameters are those for ZAP-70–mediated negative feedback regulation (table S9 and S10). Because of the uncertainty of these rate constants, we varied them over several orders of magnitude to identify their valid parameter range, in which they reproduced the correct

biological effects. These parameters should be kept in balance with those of the protective function of ZAP-70, otherwise, either biological effect could dominate, leading to the wrong conclusions. For example, if protective function of ZAP-70 dominates ZAP-70–mediated negative feedback regulation, the SILAC ratios would decrease with time, and vice versa (fig. S7D). The second set of sensitive parameters is for the Lck SH2 domain that binds to singly phosphorylated ITAMs and next processively phosphorylates the neighboring tyrosine in the ITAM. Uncertainties in these parameters are caused by the differences between the cytoplasm and membrane environments. To reproduce the experimental SILAC ratios, we find that Lck needs to have either strong kinetics in "ITAM and Lck" model or weak kinetics in the "ITAMs" model. In the "ITAM and Lck" model, Lck-SH2 strongly binds to the singly phosphorylated ITAMs (fig. S7A and table S9). If Lck-SH2 binds weakly, the experimental ratios are not reproduced (fig. S7A). Furthermore, the subsequent phosphorylation by Lck of the neighboring tyrosine in the ITAMs (while Lck-SH2 is bound to the ITAMs) requires increased kinetic parameters (fig. S7B and table S9). These high parameter values support the fact that once Lck-SH2 binds to the singly phosphorylated ITAMs, its effective concentration increases, and thus promotes the phosphorylation of the neighboring tyrosine in the ITAMs. The next sensitive parameter is the experimentally unknown binding affinity (K_D) of inhibited ZAP-70 to the doubly phosphorylated ITAMs in ZAP-70AS+Inhibitor cells (used in the ZAP-70 allosteric model). If the binding affinity (K_D) in ZAP-70AS+Inhibitor cells equals that in ZAP-70AS cells, the extent of ITAM phosphorylation in both cell types would be equal (fig. S10C and table S12). The last sensitive parameter is k_{cat}, the rate of phosphorylation of the C-terminal tyrosines of each ITAM after phosphorylation of the singly phosphorylated N-terminal tyrosines of each ITAM in the "ITAMs" model. We found that this parameter should be equal to or greater than the initial k_{cat} rate of the phosphorylation of the N-terminal tyrosines of each ITAM to reproduce the experimental SILAC ratios (fig. S8B and table S10).

Changes in multiple parameter values

Because it is nearly impossible to explore the entire parameter space, we performed sensitivity analysis by increasing or decreasing all parameters by 20% from their base values, and we performed the calculations for all computational models. We found that there were no qualitative changes in our results for all computational models.

Signaling model details

Our computational model reproduces the changes in overall ITAM phosphorylation patterns upon T cell stimulation in the absence of basal signaling. The signal strength is represented by the number of activated Lck molecules at the start of the simulations. The model includes the TCR ζ-chain ITAM with two phosphorylation sites, the N- and C-terminal tyrosines, that are sequentially phosphorylated by active Lck and sequentially dephosphorylated by the phosphatases designated "P" (for example, by CD45). In our model, we represented the three ITAMs of the ζ-chain as a single ITAM motif because the contribution of multiple ITAMs mediated signal amplification [as was shown by Dushek *et al*. (*62*)]. Thus, an addition of two other ITAMs to our model would not affect our results qualitatively. We used the following assumption in our signaling model to avoid steric hindrance between proteins, because the spacing between the N- and C-terminal tyrosine residues within one ITAM is small (about 10 to 12 amino acid residues). The following molecules cannot simultaneously bind to both tyrosines within one ITAM: two active Lck molecules with catalytic domains; the catalytic domain of

active Lck and the phosphatase P; two molecules of the phosphatase P; the catalytic domain of active Lck and one of the SH2 domains of ZAP-70; the catalytic domain of active Lck and the SH2 domain of another active Lck. The SH2 domain of active Lck and its catalytic domain can simultaneously bind to both tyrosines in an ITAM for processive phosphorylation. The binding of the SH2 domain of Lck or ZAP-70 to a phosphorylated ITAM occurs only at the vacant ITAM tyrosine sites. All reactions in the network use distributive reaction mechanisms, with the exception of the binding of Lck through its SH2 domain and its processive phosphorylation of tyrosines in the ITAM.

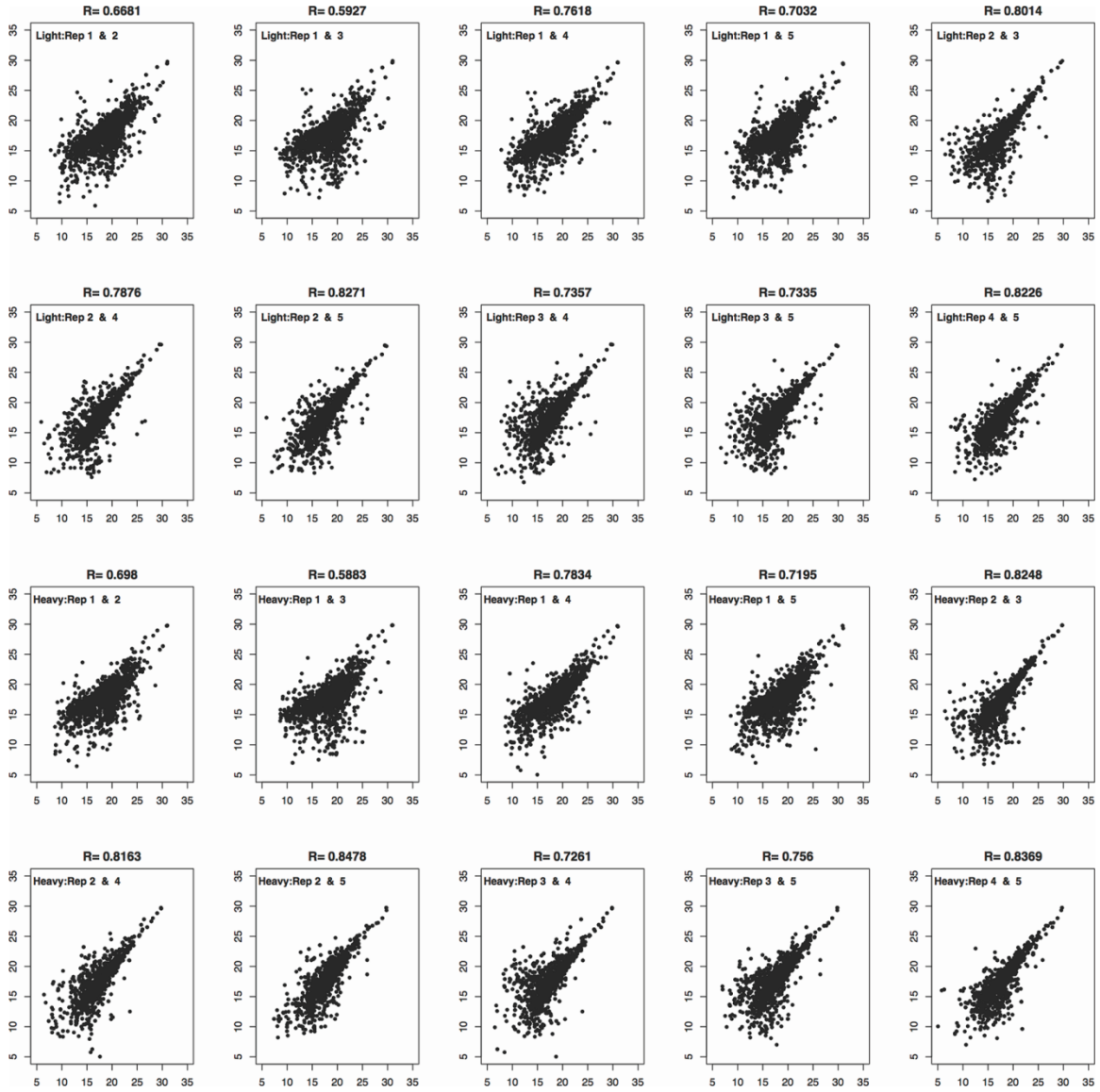

Fig. S1. Reproducibility of proteomic quantitative data in the absence of TCR stimulation. Pairwise replicate comparisons of the $\log_2$-transformed selected-ion chromatogram peak areas for individual phosphopeptides for the five sets of biological replicates in the absence of TCR stimulation (0 min samples). Each dot represents a unique quantified phosphopeptide plotted according to the peak areas in the specified two biological replicates. The plots titled "Light" show the replicate data from the cells grown in $^{12}C_6$, $^{14}N_4$ arginine, and $^{12}C_6$, $^{14}N_2$ lysine in the presence of DMSO (vehicle) for 1.5 min, whereas the plots titled "Heavy" show the replicate data from the cells grown in $^{13}C_6$, $^{15}N_4$ arginine and $^{13}C_6$, $^{15}N_2$ lysine in the presence of 10 μM HXJ42 (the ZAP-70^{AS} inhibitor) for 1.5 min.

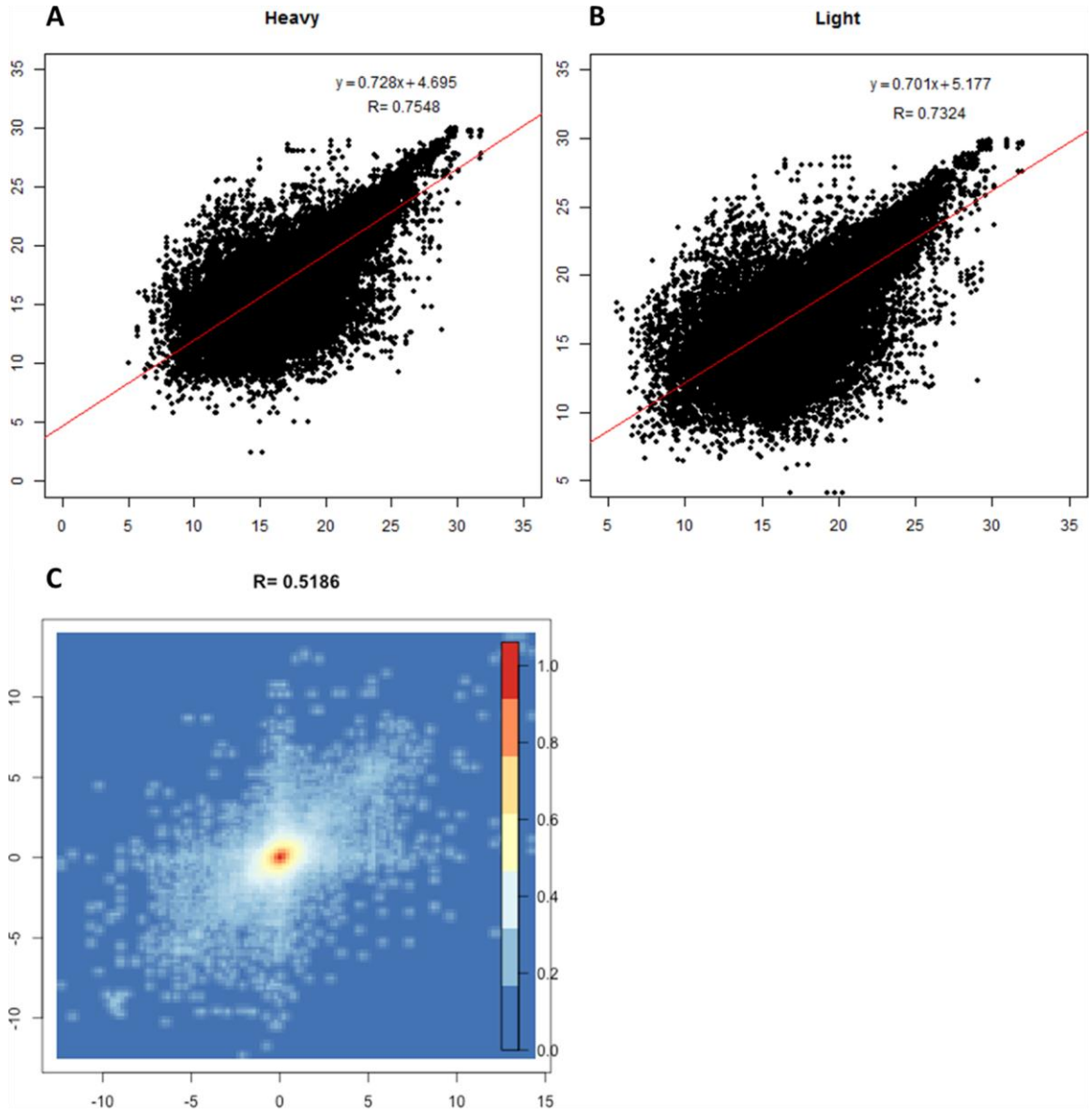

Fig. S2. Reproducibility of proteomic quantitative data for all TCR stimulation time points. Pairwise replicate comparison of the log_2-transformed selected-ion chromatogram peak areas for individual phosphopeptides for the five sets of biological replicates for all TCR stimulation timepoints (0, 2, 5, and 10 min samples). Each dot represents the detected log_2-transformed peak areas from each unique quantified phosphopeptide corresponding to two replicates from the same TCR stimulation time point. (**A**) All pairwise replicate data from the cells grown in "Light" medium ($^{12}C_6$, $^{14}N_4$ arginine, and $^{12}C_6$, $^{14}N_2$ lysine) in the presence of DMSO (vehicle) for 1.5 min. (**B**) All pairwise replicate data from the cells grown in "Heavy" medium ($^{13}C_6$, $^{15}N_4$ arginine and $^{13}C_6$, $^{15}N_2$ lysine) in the presence of 10 μM HXJ42 (the ZAP-70^{AS} inhibitor) for 1.5 min. (**C**) The pairwise comparisons of biological replicate log_2-transformed SILAC ratios (Heavy/Light) calculated from every unique phosphopeptide across all time points of TCR stimulation.

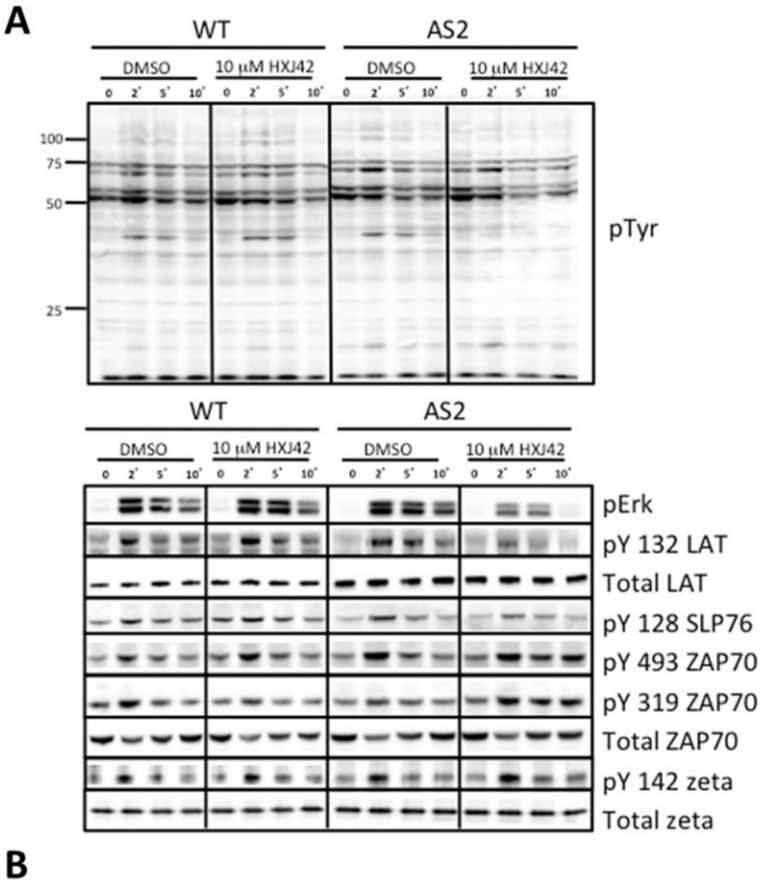

B

Phosphorylation site	Mean basal fold increase with HXJ42	Standard deviation
ZAP70 pY493	1.45	.12
Zeta pY142	1.42	.22
Lck pY394	1.29	.30

Fig. S3. Validation of inhibitor specificity. (**A**) HXK42 inhibits ZAP70-dependent signaling in ZAP70-deficient p116 cells expressing ZAP-70AS (AS2), but not wild-type (WT) ZAP-70. Whole-cell lysates from P116 cells reconstituted with WT ZAP-70 or ZAP-70AS were stimulated by crosslinking anti-CD3 and anti-CD4 antibodies in the presence or absence of 10 mM HXJ42 for the indicated times. Whole-cell lysates were analyzed by Western blotting to detect total tyrosine-phosphorylated proteins (pTyr), as well as phospho-specific sites of ERK, LAT, SLP-76, ZAP-70, and the CD3-ζ chain, as indicated. Western blots are representative of at least three independent experiments. (**B**) HXJ42 inhibits the basal phosphorylation of some proteins in unstimulated cells. Phosphorylated proteins were quantified from cells cultured in the presence or absence of the inhibitor HXJ142 and normalized to the abundance of total protein with Image Lab 5.2 software (Bio-Rad). Data are means ± SD from three separate experiments. For pY493, $P < 0.05$; for pY142, $P = 0.08$; for pY394, $P > 0.18$.

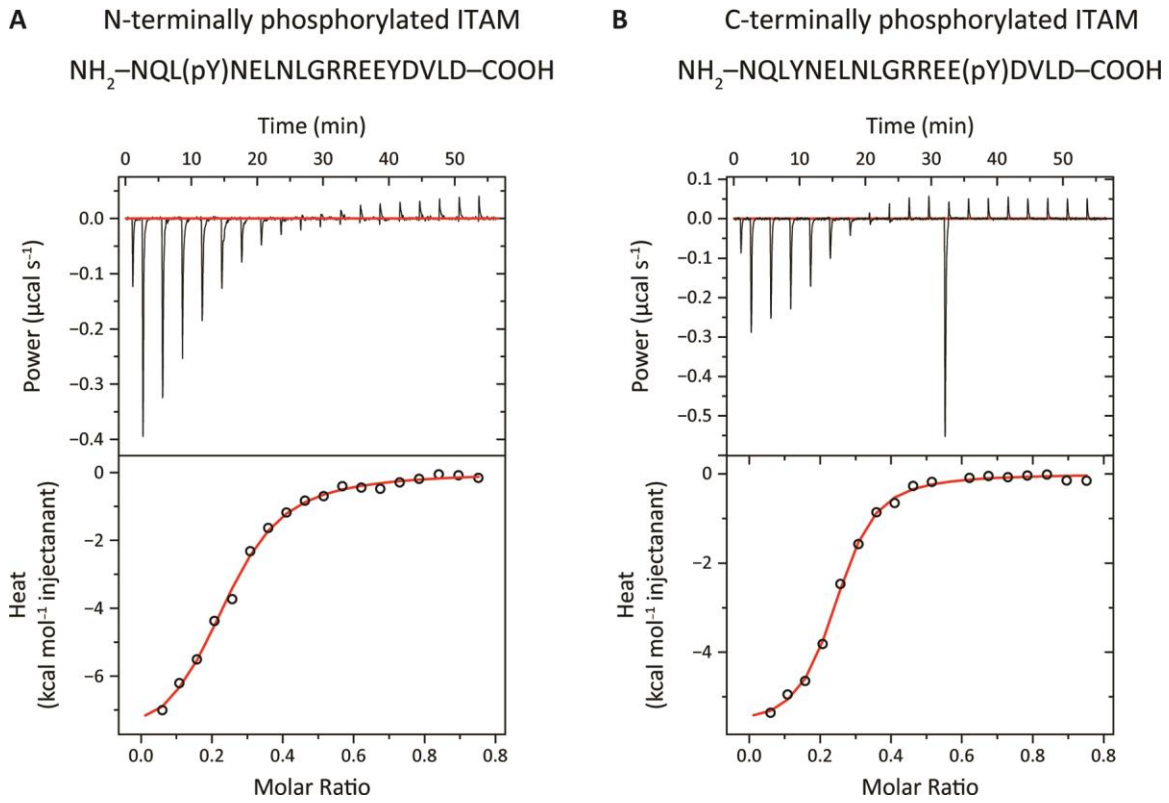

Fig. S4. Binding of the SH2 domain of Lck to monophosphorylated TCR ζ-chain ITAM peptides. (**A** and **B**) ITC was used to determine the binding affinity of the isolated SH2 domain of human Lck (amino acid residues 126 to 223) to monophosphorylated peptides corresponding to the N-terminal ITAM of human TCR ζ (residues 69 to 87, numbering including the signal peptide). The peptides were phosphorylated on either (A) the N-terminal tyrosine or (B) the C-terminal tyrosine. Binding thermograms (top) and isotherms with fits from a one-set-of-sites binding model (bottom) for two representative experiments at 25°C are shown. The heat of the first injection for both runs and that of the twelfth injection from the C-terminally phosphorylated peptide run were omitted from the fitting. A constant value of 0.75 kcal mol^{-1}, chosen based on the goodness of fit, was subtracted from the integrated heats in both runs to bring the baseline heat of dilution to zero. The Lck SH2 domain was the syringe titrant, at 359 µM, and the peptide was the cell reactant, at 30 µM. The apparent binding parameters from fits to the data for these individual runs are presented in table S4. Deviation of the stoichiometry parameter *n* from a value of 1 reflects inaccuracy in the measured peptide concentration. The fitted values of the association constant and molar enthalpy change upon binding do not depend on *n*.

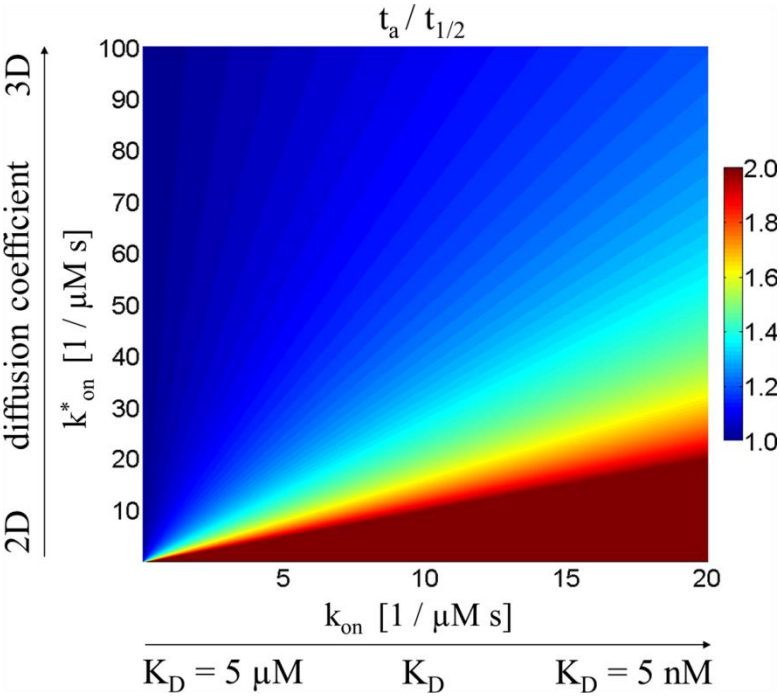

Fig. S5. The number of rebinding events between enzyme and substrate upon variation of different kinetic parameters. An estimation of the number of enzyme-substrate rebinding events upon moving from the membrane environment (2D case) to the cytoplasm environment (3D case) with increasing substrate binding affinity (K_D).

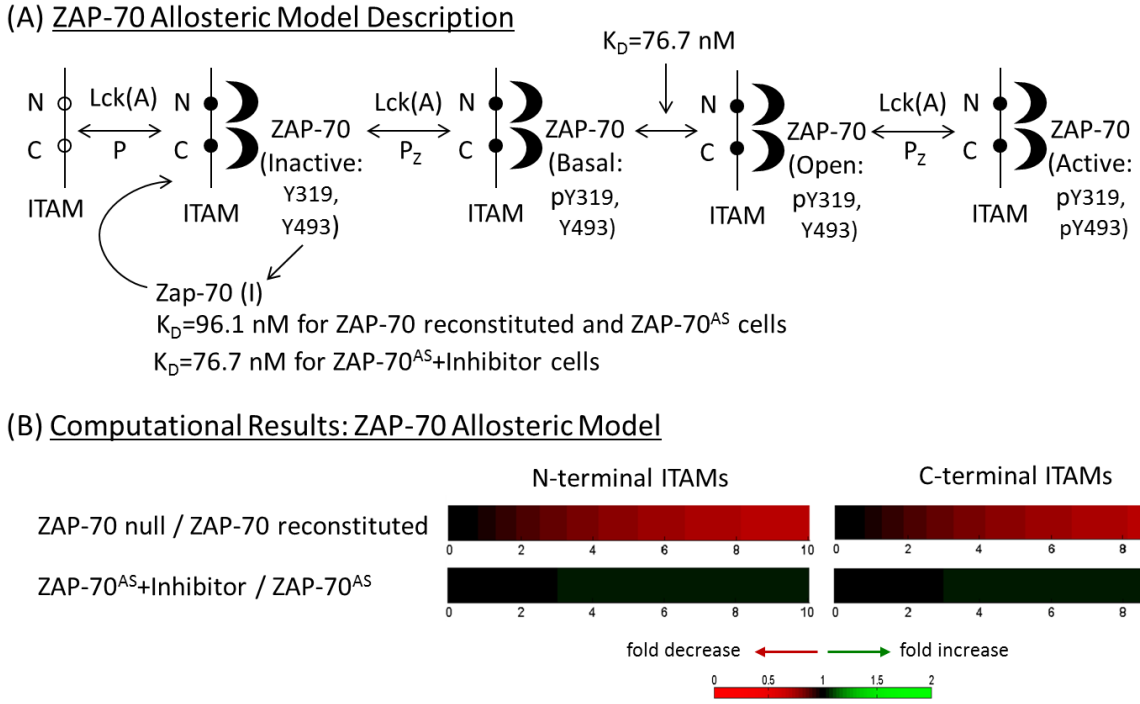

Fig. S6. Description of the ZAP-70 allosteric model and the results of calculations with this model. (**A**) Description of ZAP-70 allosteric model. In the model of the ZAP-70 reconstituted cells and the ZAP-70AS cells, the autoinhibited ZAP-70 binds to the doubly phosphorylated ITAMs with a reduced affinity (K_D = 96.1 nM). Next, active Lck phosphorylates the tyrosine residues Y315 and Y319 in the SH2-linker domain of ZAP-70, leading to a conformational change (to its open state), and therefore to an increase in the ZAP-70 binding affinity (K_D = 76.7 nM). Later, active Lck phosphorylates the ZAP-70 catalytic domain, generating active ZAP-70. The model of the ZAP-70AS+Inhibitor cells keeps ZAP-70 in its autoinhibited conformation with an increased binding affinity (K_D = 76.7 nM). (**B**) The results of calculations using the ZAP-70 allosteric model for the SILAC ratios of the N- and C- terminal tyrosines within each ITAM as a ratio heatmap.

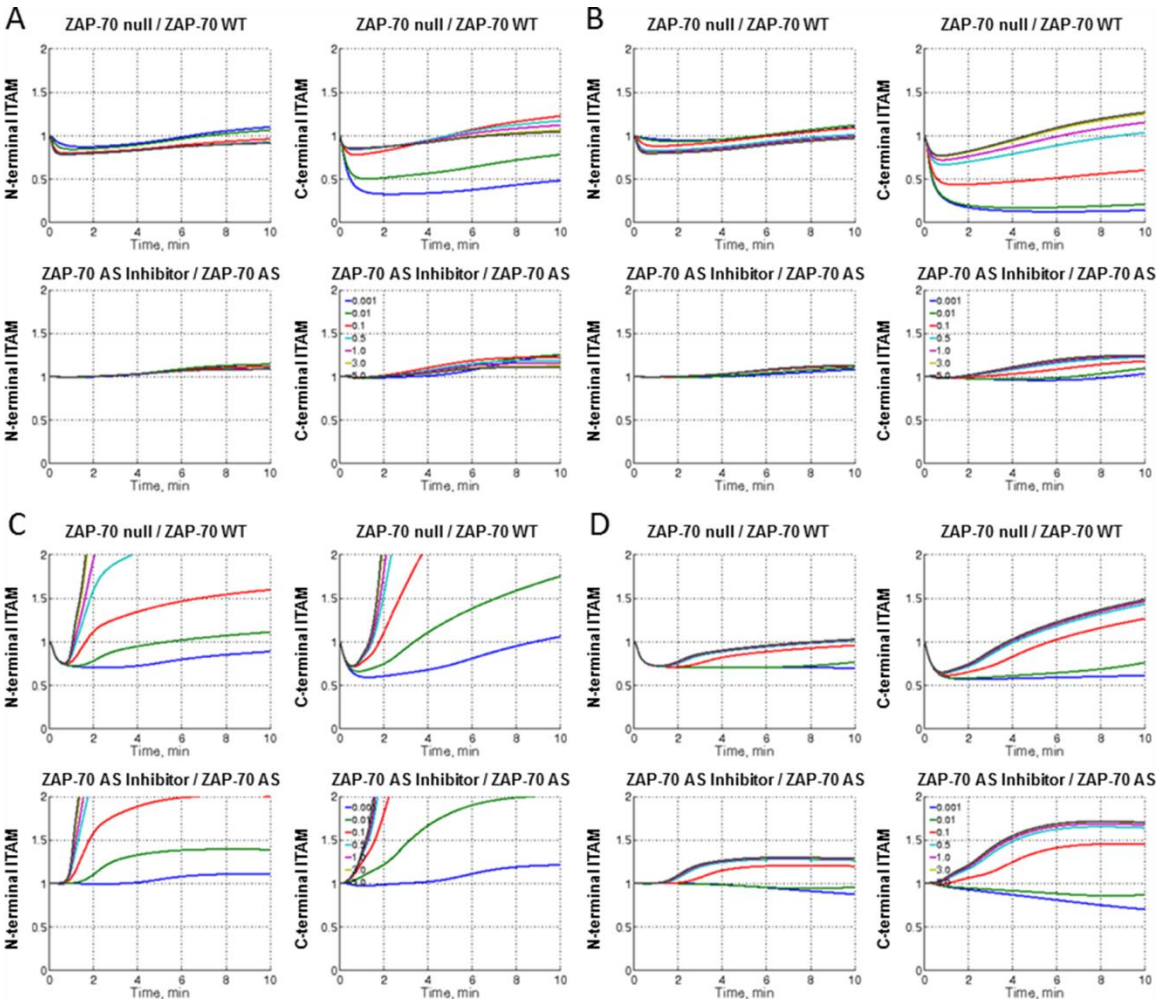

Fig. S7. Sensitivity analysis of the kinetic parameters used in calculations for the "ITAM and Lck" model. The variation of kinetic parameters for every chemical reaction was in the following parameter range: 0.001, 0.01, 0.1, 0.5, 1.0, 3.0, and 5.0 s^{-1}. (**A**) Sensitivity analysis for varying the rate of binding (k_{on}) of Lck-SH2 to the singly phosphorylated tyrosine residue of N-terminal ITAMs; that is, the Lck(A) + ITAM(N_p,C_0) ↔ [Lck(A, SH2):ITAM(N_p,C_0)] reaction. For the ZAP-70 null / ZAP-70 reconstituted SILAC ratio (top): at low rates, the ZAP-70 null / ZAP-70 reconstituted ratio for C-terminal ITAM tyrosines is lower than that for the N-terminal ITAM tyrosines, whereas at high rates, asymmetrical ITAM tyrosine phosphorylation is reproduced. For the ZAP-70^{AS}+Inhibitor / ZAP-70^{AS} SILAC ratio (bottom), there is no qualitative change. (**B**) Sensitivity analysis for varying the rate of binding (k_{on}) of Lck to the C-terminal ITAM tyrosines while bound with its SH2 domain to singly phosphorylated N-terminal ITAM tyrosines; that is, the [Lck(A,SH2):ITAM(N_p,C_0)] ↔ [Lck(A,SH2):ITAM(N_p,C_0):Csite] reaction. For the ZAP-70 null / ZAP-70 reconstituted SILAC ratio (top): at low rates, the ZAP-70 null / ZAP-70 reconstituted ratio for C-terminal ITAM tyrosines is lower than that for N-terminal ITAM tyrosines, whereas at high rates, asymmetrical ITAM tyrosine phosphorylation is reproduced. For the ZAP-70^{AS}+Inhibitor / ZAP-70^{AS} SILAC ratio (bottom), there is no qualitative change. These parameters support the observation that, once Lck-SH2 binds to the singly phosphorylated ITAMs, the effective concentration of Lck increases, which thus promotes the phosphorylation of the neighboring sites of the ITAMs. (**C**) Sensitivity analysis for varying

the rate of binding (k_{on}) of the ZAP-70–bound ITAM complex to active Lck; that is, the Lck(A) + [ITAM(N_p,C_p):Z(A)] ↔ [Lck(A):ITAM(N_p,C_p):Z(A)] reaction. For both SILAC ratios: at high rates, negative feedback dominates, whereas at low rates, the experimental trends are reproduced. (**D**) Sensitivity analysis for varying the rate (k_{cat}) for the ZAP-70–dependent negative feedback regulation of Lck at Y192; that is, the [Lck(A):ITAM(N_p,C_p):Z(A)] → Lck(I) + [ITAM(N_p,C_p):Z(A)] reaction. For both SILAC ratios: at low rates, the protective function of ZAP-70 dominates, whereas at high rates, the negative feedback dominates and the experimental trends are reproduced.

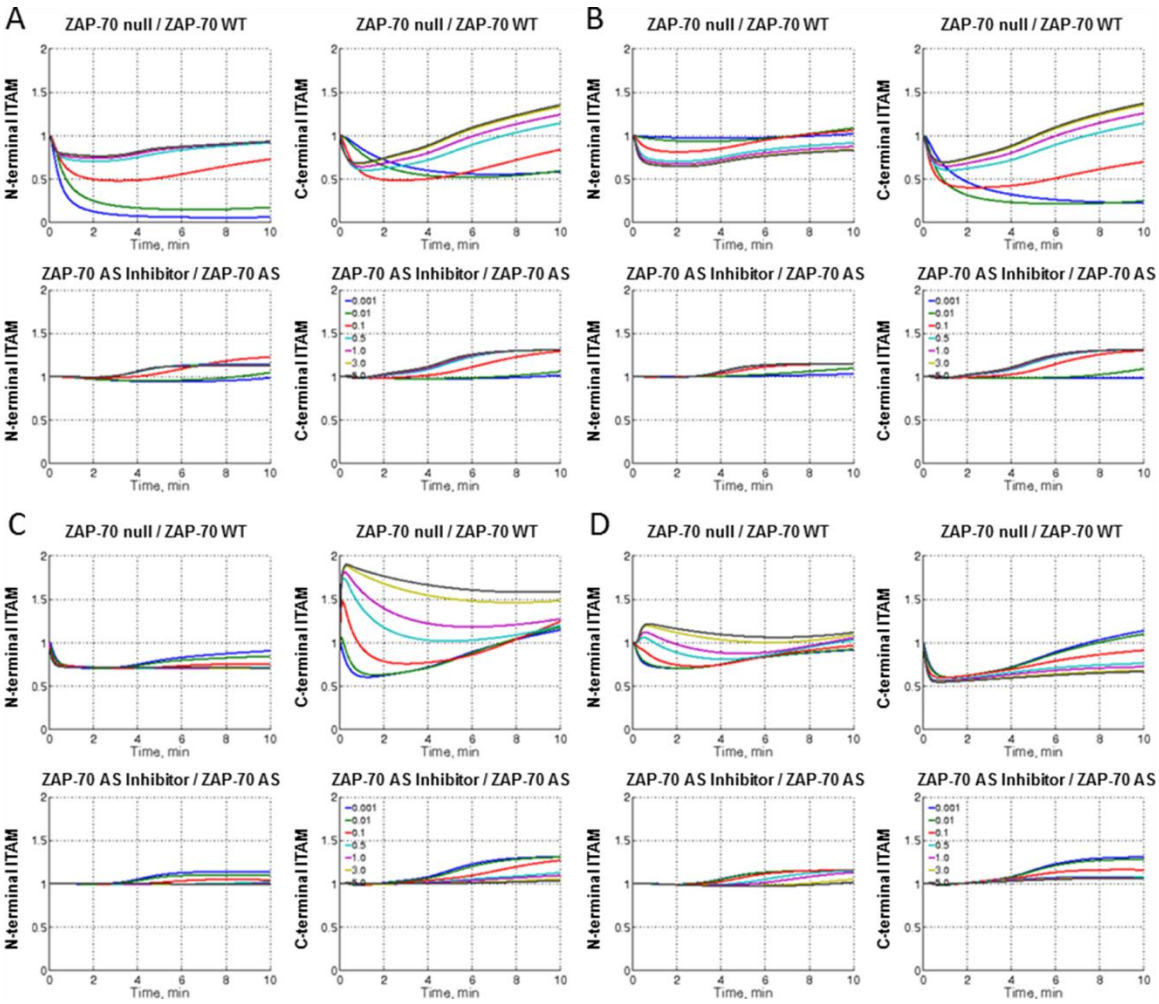

Fig. S8. Sensitivity analysis of the kinetic parameters used in calculations for the "ITAMs" model. The variation of kinetic parameters for every chemical reaction was in the following parameter range: 0.001, 0.01, 0.1, 0.5, 1.0, 3.0, and 5.0 s^{-1}. (**A**) Sensitivity analysis for varying the rate of production (k_{cat}) of singly phosphorylated N-terminal ITAM tyrosines; that is, the [Lck(A, Nsite):ITAM(N_0,C_0)] → Lck(A) + ITAM(N_p,C_0) reaction. For the ZAP-70 null / ZAP-70 reconstituted SILAC ratio (top): at low rates, asymmetrical ITAM tyrosine phosphorylation is not reproduced, whereas at low rates, the ZAP-70 null / ZAP-70 reconstituted ratio for N-terminal ITAM tyrosines is lower than that for C-terminal ITAM tyrosines, because k_{cat} for the phosphorylation of C-terminal ITAM tyrosines is greater. For the ZAP-70^{AS}+Inhibitor / ZAP-70^{AS} SILAC ratio (bottom), there is no qualitative change. (**B**) Sensitivity analysis for varying the rate of production (k_{cat}) of doubly phosphorylated ITAM tyrosines from singly phosphorylated N-terminal ITAM tyrosines; that is, the [Lck(A):ITAM(N_p,C_0)] → Lck(A) + ITAM(N_p,C_p) reaction. For the ZAP-70 null / ZAP-70 reconstituted SILAC ratio (top): at low rates, asymmetrical ITAM tyrosine phosphorylation is not reproduced, whereas at low rates, the ZAP-70 null / ZAP-70 reconstituted ratio for N-terminal ITAM tyrosines is greater than that for C-terminal ITAM tyrosines. For the ZAP-70^{AS}+Inhibitor / ZAP-70^{AS} SILAC ratio (bottom), there is no qualitative change. (**C**) Sensitivity analysis for varying the rate of binding (k_{on}) of ZAP-70 to singly phosphorylated N-terminal ITAMtyrosines; that is, the ITAM(N_p,C_0) + Z → [ITAM(N_p,C_0):Z] reaction. For the ZAP-70 null / ZAP-70 reconstituted SILAC ratio (top): at

low rates, there is no qualitative change, whereas at high rates, ZAP-70 protects singly phosphorylated N-terminal ITAM tyrosines from dephosphorylation by phosphatases, which results in decreased phosphorylation of C-terminal ITAM tyrosines in ZAP-70–reconstituted cells. For the ZAP-70^{AS}+Inhibitor / ZAP-70^{AS} SILAC ratio (bottom), there is no qualitative change. (**D**) Sensitivity analysis for varying the rate of binding (k_{on}) of ZAP-70 to singly phosphorylated C-terminal ITAM tyrosines; that is, the ITAM(N_0,C_p) + Z → [ITAM(N_0,C_p):Z] reaction. For the ZAP-70 null / ZAP-70 reconstituted SILAC ratio (top): at low rates, there is no qualitative change, whereas at high rates, ZAP-70 protects singly phosphorylated C-terminal ITAM tyrosines from dephosphorylation by phosphatases, which results in decreased phosphorylation of N-terminal ITAM tyrosines in ZAP-70–reconstituted cells. For the ZAP-70^{AS}+Inhibitor / ZAP-70^{AS} SILAC ratio (bottom), there is no qualitative change.

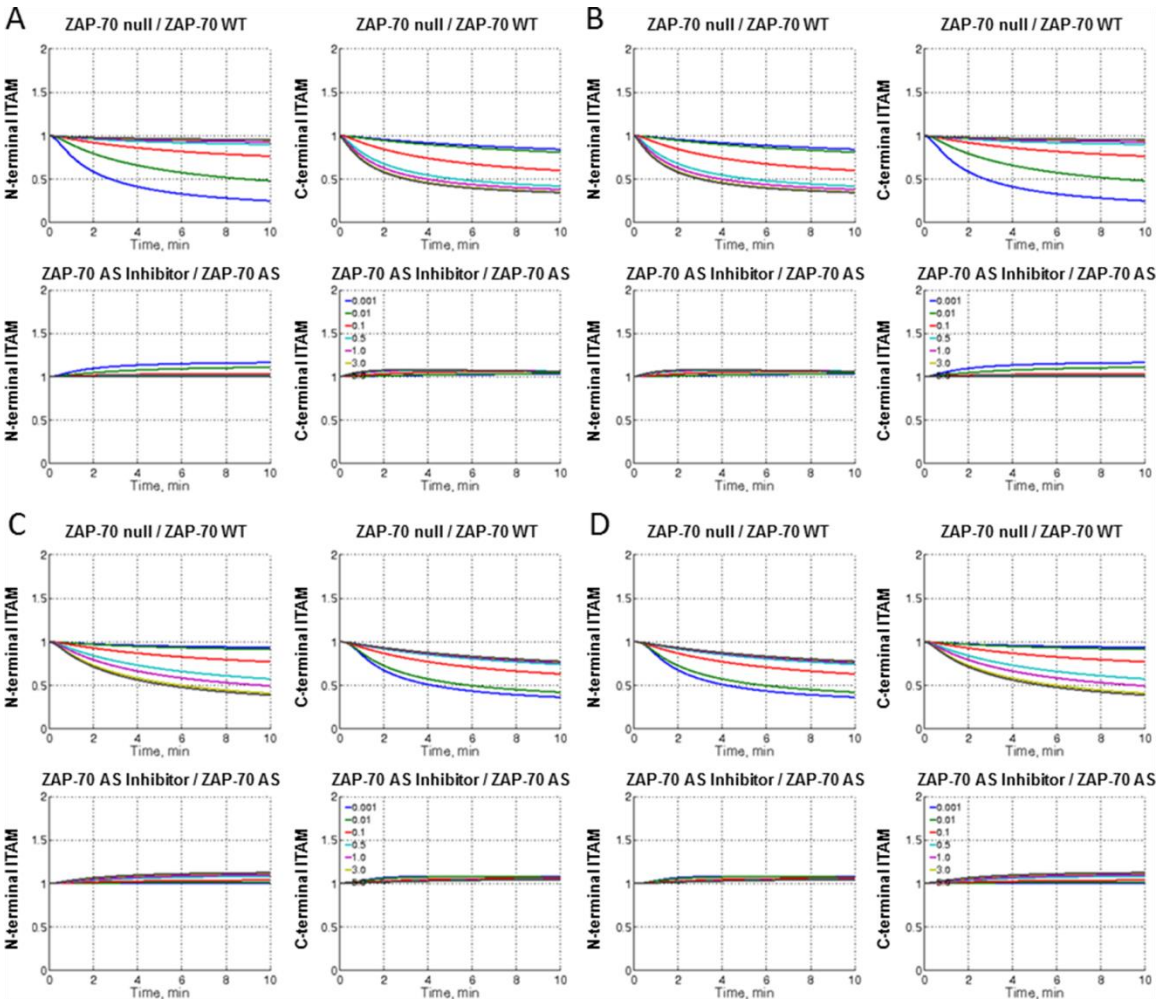

Fig. S9. Sensitivity analysis of the kinetic parameters used in calculations for the ZAP-70 allosteric model (part I). The variation of kinetic parameters for every chemical reaction was in the following parameter range: 0.001, 0.01, 0.1, 0.5, 1.0, 3.0, and 5.0 s^{-1}. (**A**) Sensitivity analysis for varying the rate of production (k_{cat}) of singly phosphorylated N-terminal ITAM tyrosines; that is, the [Lck(A, Nsite):ITAM(N_0,C_0)] → Lck(A) + ITAM(N_p,C_0) reaction. For the ZAP-70 null / ZAP-70 reconstituted SILAC ratio (top): at low rates, there is no qualitative change, whereas at high rates, the ZAP-70 null / ZAP-70 reconstituted SILAC ratio for the N-terminal ITAM tyrosine is higher than that of the C-terminal ITAM tyrosine. For the $ZAP\text{-}70^{AS}$+Inhibitor / $ZAP\text{-}70^{AS}$ SILAC ratio (bottom), there is no qualitative change. (**B**) Sensitivity analysis for varying the rate of production (k_{cat}) of singly phosphorylated C-terminal ITAM tyrosines; that is, the [Lck(A, Csite):ITAM(N_0,C_0)] → Lck(A) + ITAM(N_0,C_p) reaction. For the ZAP-70 null / ZAP-70 reconstituted SILAC ratio (top): at low rates, there is no qualitative change, whereas at high rates, the ZAP-70 null / ZAP-70 reconstituted SILAC ratio for the C-terminal ITAM tyrosines is greater than that for the N-terminal ITAM tyrosines. For the $ZAP\text{-}70^{AS}$+Inhibitor / $ZAP\text{-}70^{AS}$ SILAC ratio (bottom): there is no qualitative change. (**C**) Sensitivity analysis for varying the rate of dephosphorylation (k_{cat}) of singly phosphorylated N-terminal ITAM tyrosines to its unphosphorylated form by phosphatases; that is, the [ITAM(N_p,C_0):P] → ITAM(N_0,C_0) + P reaction. For the ZAP-70 null / ZAP-70 reconstituted SILAC ratio (top): at low rates, there is no qualitative change, whereas at high rates, the ZAP-70 null / ZAP-70 reconstituted SILAC ratio

for the C-terminal ITAM tyrosines is greater than that for the N-terminal ITAM tyrosines. For the ZAP-70AS+Inhibitor / ZAP-70AS SILAC ratio (bottom), there is no qualitative change. (**D**) Sensitivity analysis for varying the rate of dephosphorylation (k_{cat}) of singly phosphorylated C-terminal ITAM tyrosines to their unphosphorylated form by phosphatases; that is, the [ITAM(N_0,C_p):P] → ITAM(N_0,C_0) + P reaction. For the ZAP-70 null / ZAP-70 reconstituted SILAC ratio (top): at low rates, there is no qualitative change, whereas at high rates, the ZAP-70 null / ZAP-70 reconstituted SILAC ratio for the N-terminal ITAM tyrosines is greater than that for the C-terminal ITAM tyrosines. For the ZAP-70AS+Inhibitor / ZAP-70AS SILAC ratio (bottom), there is no qualitative change.

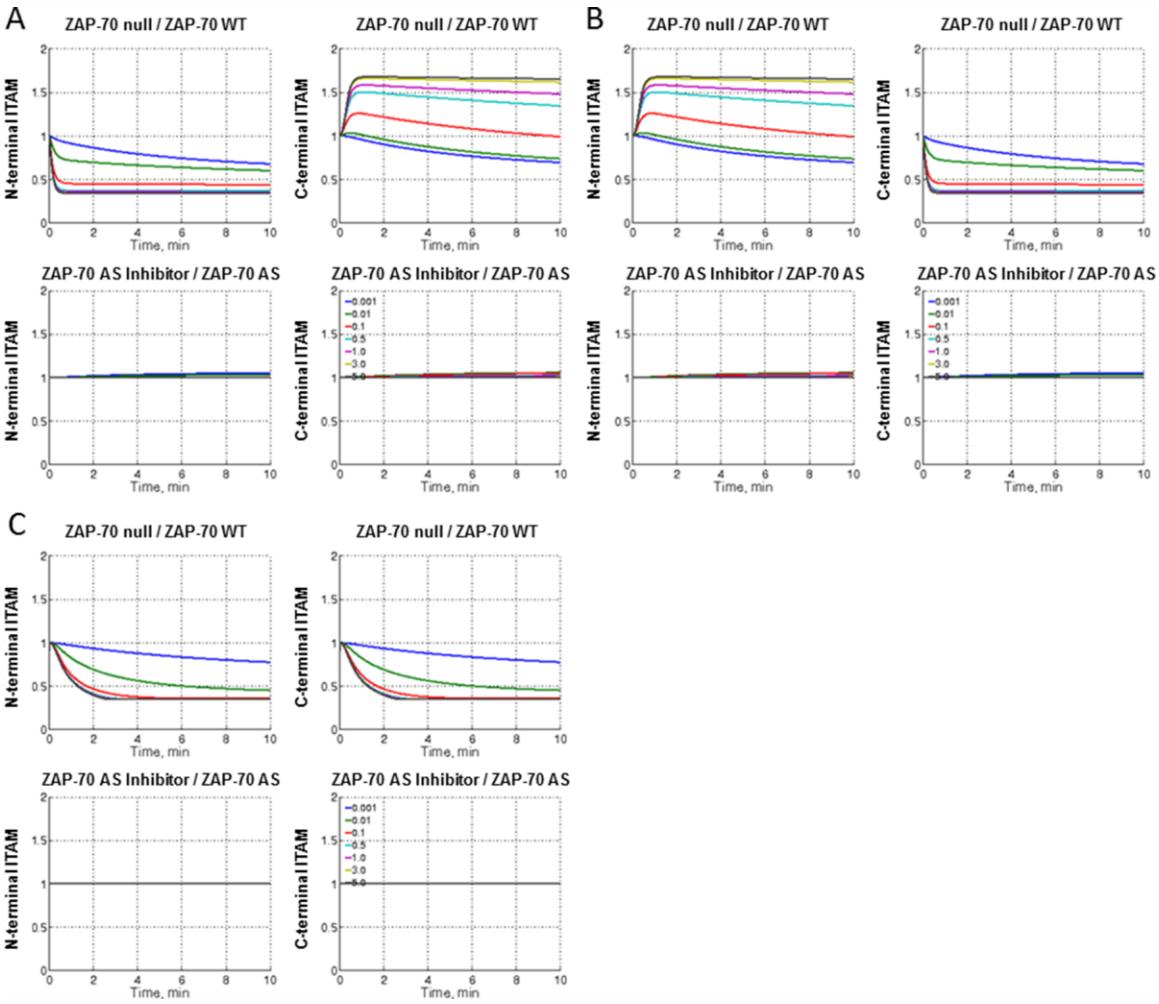

Fig. S10. Sensitivity analysis of the kinetic parameters used in calculations for the ZAP-70 allosteric model (part II). The variation of kinetic parameters for every chemical reaction was in the following parameter range: 0.001, 0.01, 0.1, 0.5, 1.0, 3.0, and 5.0 s^{-1}. (**A**) Sensitivity analysis for varying the rate of binding (k_{on}) of ZAP-70 to singly phosphorylated N-terminal ITAM tyrosines; that is, the ITAM(N_p,C_0) + Z → [ITAM(N_p,C_0):Z] reaction. For the ZAP-70 null / ZAP-70 reconstituted SILAC ratio (top): at low rates, there is no qualitative change, whereas at high rates, ZAP-70 protects singly phosphorylated N-terminal ITAM tyrosines from dephosphorylation by phosphatases, which results in an increased production of phosphorylated C-terminal ITAM tyrosines. For the ZAP-70^{AS}+Inhibitor / ZAP-70^{AS} SILAC ratio (bottom), there is no qualitative change. (**B**) Sensitivity analysis for varying the rate of binding (k_{on}) of ZAP-70 to the singly phosphorylated C-terminal ITAM tyrosines; that is, the ITAM(N_0,C_p) + Z → [ITAM(N_0,C_p):Z] reaction. For the ZAP-70 null / ZAP-70 reconstituted SILAC ratio (top): at low rates, there is no qualitative change, whereas at high rates, ZAP-70 protects singly phosphorylated C-terminal ITAM tyrosines from dephosphorylation by phosphatases, which results in an increased production of phosphorylated N-terminal ITAM tyrosines. For the ZAP-70^{AS}+Inhibitor / ZAP-70^{AS} SILAC ratio (bottom), there is no qualitative change. (**C**) Sensitivity analysis for varying the rate of binding (k_{on}) of ZAP-70 to doubly phosphorylated ITAMs; that is, the ITAM(N_p,C_p) + Z → [ITAM(N_p,C_p):Z] reaction. For the ZAP-70 null / ZAP-70 reconstituted SILAC ratio (top): at low rates, there is no qualitative change, whereas at high

rates, ZAP-70 protects doubly phosphorylated ITAM tyrosines from dephosphorylation by phosphatases. If the binding affinity (K_D) of ZAP-70 to the doubly phosphorylated ITAMs of ZAP-70^{AS}+Inhibitor cells is equal to that of the ZAP-70^{AS} cells, the experimental data for the ZAP-70^{AS}+Inhibitor / ZAP-70^{AS} SILAC ratio are not reproduced (bottom).

Table S1. Complete list of sequence and phosphorylation site assignments of all identified phosphopeptides with corresponding SIC peak areas and statistics, protein accession numbers, gene ontology, and KEGG functional annotation. Included in this table are confident MS/MS peptide assignments at >20 MOWSE score, <2 ppm mass error, and logistic score filter to achieve a final estimated 1% FDR by decoy database approach. Only forward database hits are included in this table.

Table S2. Complete list of phosphopeptides detected from every replicate and time point of TCR stimulation. Included in these tables are all phosphotyrosine containing peptides with MOWSE score >20 and mass error <2 ppm, including decoy database reversed sequence hits. Reversed decoy database hits, if any, for each replicate and time point are labeled with protein descriptor ###REV### and an "R" designation in database direction. A reversed hit represents peptide spectrum matches to the nonsense, reversed protein sequences that do not match the correct, normal protein sequences that are used to estimate the FDR of the peptide sequences across experiments. Listed are the assigned names of the corresponding proteins, the position of the phosphorylation site within the protein sequences, and the assigned peptide sequence. For the peptide sequence, * represents phosphorylation, and # represents Met oxidation. Every reported peptide includes the Logistic Spectral Validation score and Mascot Mowse score, which reflect confidence in the sequence assignment, and the Ascore, which reports the confidence in the localization of the phosphorylation site. Also reported is the mass error in ppm, the isolated mass of the peptide, the charge state, and the scan number.

Table S3. Fold change between HXJ-42–treated and DMSO-treated ZAP-70AS cells and *Q* values for the peptides listed in Table 1. The numbers in bold represent the *Q* values less than the threshold of 0.05 (5% FDR) used in this study.

		0 min		2 min		5 min		10 min	
Protein name	**Phosphosite annotated**	**Fold change**	***Q* value**	**Fold change**	***Q* value**	**Fold change**	***Q* value**	**Fold change**	***Q* value**
ATP6V1E	Y56	1.2	0.294	2.3	0.068	**1.6**	**0.031**	1.3	0.224
CblB	Y665	2.6	0.356	-3.2	0.051	**-2.5**	**0.043**	1.2	0.490
CD28	Y191*	1.1	0.442	**-1.4**	**0.049**	-1.2	0.124	-1.2	0.256
CD28	Y206Y209*	**-2.1**	**0.036**	-1.7	0.190	1.6	0.469	-1.4	0.109
CD3E	Y199*	1.0	0.488	**1.2**	**0.039**	1.2	0.056	1.5	0.139
CD3 ζ	Y64Y72*	1.2		-2.7	0.071	**-2.3**	**0.038**	-1.5	0.172
CD3 ζ	Y72*	1.3	0.350	1.2	0.104	2.0	0.161	**1.7**	**0.028**
CD3 ζ	Y83*	1.1	0.269	1.3	0.105	**1.2**	**0.023**	1.4	0.070
CD3 ζ	Y111*	1.1	0.317	**1.3**	**0.037**	**1.2**	**0.030**	1.5	0.095
CD3 ζ	Y123*	1.2		1.6	0.176	1.3	0.499	1.7	0.119
CD3 ζ	Y142*	1.1	0.349	**1.2**	**0.048**	2.1	0.277	2.0	0.349
CD3 ζ	Y142*	1.0	0.489	1.2	0.071	1.1	0.105	1.4	0.167
CD3 ζ	Y142*	1.0	0.489	1.2	0.071	1.1	0.105	1.4	0.167
CD3 ζ	Y153*	**-1.5**	**0.046**	-2.0	0.074	1.0	0.510	1.9	0.264
CD3 δ	Y149Y160*	1.2	0.219	**1.5**	**0.016**	**1.5**	**0.030**	1.8	0.090
CD3 δ	Y149*	1.2	0.141	1.3	0.069	**1.4**	**0.044**	**1.8**	**0.020**
CD3 δ	Y149S161*	1.1	0.364	**1.6**	**0.035**	**1.5**	**0.016**	1.9	0.092
CD3 δ	Y160*	-1.0	0.460	**1.2**	**0.045**	1.2	0.054	1.5	0.105
ERK1	T202Y204*	-2.7		-2.7	0.248	-7.0		**-12.3**	**0.027**
ERK1	Y204*	-8.5		**-7.1**	**0.044**	-5.1	0.153	-7.5	0.069
ERK2	T185Y187*	-3.3		**-13.1**	**0.034**	-7.9	0.167	**-8.3**	**0.044**
ERK2	T185Y187*	-3.3		**-13.1**	**0.034**	-7.9	0.167	**-8.3**	**0.044**
ERK2	Y187*	1.6	0.280	**-4.7**	**0.038**	-4.5	0.114	**-5.4**	**0.033**
ERK2	Y187*	1.6	0.280	**-4.7**	**0.038**	-4.4	0.050	**-5.4**	**0.033**

GSK3B	Y71	-1.0	0.447	-1.3	0.241	**-2.7**	**0.012**	-2.5	0.101
ITK	Y146	-2.3	0.155	**-10.6**	**0.046**	-1.6	0.288	-2.7	0.073
ITK	Y512*	-1.2	0.297	**-2.0**	**0.028**	-1.4	0.054	-1.2	0.241
Lck	Y192*	**-8.3**	**0.001**	**-6.9**	**0.011**	**-7.3**	**0.007**	**-7.0**	**0.005**
Lck	Y394*	1.3	0.500	1.1	0.440	1.3	0.168	**1.6**	**0.040**
Lck	Y470	1.0	0.501	9.3	0.130	**7.6**	**0.013**	1.1	0.146
MAPK14	T180Y182*	1.4	0.104	**-3.4**	**0.044**	-2.6	0.169		
NCK1	Y105*	**-70.7**	**0.022**	-2.8	0.141	-4.0	0.209	-4.5	0.135
PI3K regulatory α	Y467*	1.1	0.052	1.2		1.2	0.071	**1.2**	**0.033**
PI3K regulatory γ	Y199	-1.7	0.097	-1.4	0.174	**-1.5**	**0.023**	-1.4	0.116
RXR-alpha	Y150	-1.6		-1.6	0.224	-1.2	0.286	**-1.3**	**0.036**
PLCγ1	Y771*	-1.1	0.388	**-2.4**	**0.031**	**-1.8**	**0.044**	-1.6	0.122
SHP-1	S556Y564*	1.5	0.306	-2.8	0.071	-2.5	0.079	**-2.4**	**0.045**
SHP-2	Y62*	**-1.3**	**0.007**	-1.3	0.173	-1.6	0.203	-1.2	0.060
PYK2	Y579*	**7.4**	**0.027**	**35.3**	**0.017**	**35.0**	**0.001**	**36.3**	**0.012**
PYK2	Y579Y580*	1.2	0.486	1.7	0.331	1.5	0.248	**2.4**	**0.043**
PYK2	Y580*	**23.6**	**0.036**	8.5	0.051	13.4	0.105	21.2	0.071
Tec	Y519	1.2	0.519	**-2.2**	**0.023**	-1.3	0.156	-1.2	0.270
VAV1	Y791	-1.2	0.288	**-3.0**	**0.017**	-1.8	0.105	-1.7	0.069
VAV3	Y265	1.5	0.380	-1.7	0.255	**-2.6**	**0.028**	-1.7	0.169
ZAP70	T286Y292*	-1.5	0.168	**-7.2**	**0.023**	**-6.6**	**0.032**	**-4.9**	**0.033**
ZAP70	S289Y292*	-1.5	0.168	**-7.2**	**0.023**	**-6.6**	**0.032**	**-4.9**	**0.033**
ZAP70	Y292*	-1.0	0.467	**-1.5**	**0.037**	**-1.6**	**0.044**	1.1	0.509
ZAP70	S301Y319	1.2	0.368	**1.1**	**0.045**	-1.0	0.446	1.6	0.295
ZAP70	Y315Y319	1.2	0.361	**1.1**	**0.045**	1.0	0.513	23.6	0.295
ZAP70	S491Y493*	-1.0	0.430	**2.0**	**0.001**	**1.7**	**0.012**	2.2	0.116
ZAP70	Y492Y493*	-1.0	0.470	**2.0**	**0.001**	**1.8**	**0.019**	2.4	0.125
ZAP70	Y493*	1.1	0.461	**2.6**	**0.022**	**2.2**	**0.040**	2.4	0.080

ZAP70	Y597Y598	1.0	0.522	-1.8	0.064	**-2.6**	**0.030**	-1.6	0.147
ZAP70	Y597	-1.1	0.363	-1.4	0.195	**-1.9**	**0.044**	-1.4	0.140
ZAP70	Y597Y598	1.3	0.305	-1.6	0.080	**-2.4**	**0.045**	-1.5	0.199
ZAP70	Y597S599	1.3	0.305	-1.6	0.080	**-2.4**	**0.045**	-1.5	0.199
ZAP70	Y598	1.2	0.068	-1.1	0.139	**-1.4**	**0.045**	-1.2	0.267

Table S4. Binding parameters for the Lck SH2 domain and monophosphorylated ζ ITAM peptides determined by isothermal titration calorimetry at 25°C. All reported parameters are apparent values obtained by fitting a one-set-of-sites binding model to the results of a single representative ITC experiment. n, stoichiometry; K_A, association constant; K_D, dissociation constant; ΔH^o, molar enthalpy of binding; $T\Delta S^o$, molar entropy of binding × 298 K.

Peptide sequence	n[a]	K_A (M^{-1})	K_D (μM)	ΔH^o (cal mol^{-1})	$T\Delta S^o$ (cal mol^{-1})
NQL(pY)NELNLGRREEYDVLD	0.596 ± 0.013[b]	$3.82\times10^5 \pm 4.0\times10^4$	2.6 ± 0.3	−8259 ± 244	−644
NQLYNELNLGRREE(pY)DVLD	0.59 ± 0.007	$9.75\times10^5 \pm 9.6\times10^4$	1.0 ± 0.1	−5745 ± 95	2426

[a]Deviation from the value of 1 for the stoichiometry parameter is primarily a result of inaccurately measured peptide concentrations. [b]Uncertainty is given as the SEM from the nonlinear least squares fitting.

Table S5. Concentrations of species used in calculations for all models (volume = 1 μm^3). Lck(A) represents active Lck; ITAM(N_0,C_0) indicates unphosphorylated ITAMs; P represents phosphatases that dephosphorylate singly or doubly phosphorylated ITAMs; Z represents ZAP-70; P_z indicates phosphatases that dephosphorylate basal and active ZAP-70; P_{Lck} represents phosphatases that dephosphorylate inactive Lck. P_{Lck} is absent in the ZAP-70 protective function (Fig. 5, "ZAP-70 Bind") and ZAP-70 allosteric models (fig. S6).

Species	No. of molecules in V
Lck(A)	1000
ITAM(N_0,C_0)	1000
P	2000
Z	500
P_z	500
P_{Lck}	500

Table S6. Reactions and kinetic parameters used in calculations for the ZAP-70–mediated negative feedback model and models used to reproduce an asymmetry in ITAM phosphorylation. Lck molecules exist in two states: active Lck and inactive Lck, which are presented as Lck(A) and Lck(I), respectively. Lck(A, SH2) denotes the noncatalytic SH2 domain of Lck. ITAM(N_0,C_0), ITAM(N_p,C_0), ITAM(N_0,C_p), and ITAM(N_p,C_p) denote unphosphorylated ITAMs, the singly phosphorylated N-terminal tyrosine of ITAMs, the singly phosphorylated C-terminal tyrosine of ITAMs, and doubly phosphorylated ITAM tyrosines, respectively. ZAP-70 molecules exist in three states: inactive ZAP-70, basal ZAP-70, and fully active ZAP-70, which are labeled as Z, Z(B), and Z(A), respectively.

Reactions	**k_{on}, molec^{-1} s^{-1}**	**k_{off}, s^{-1}**	**k_{cat}, s^{-1}**	**Reference**
Lck(A) + ITAM(N_0,C_0) ↔ [Lck(A, Nsite):ITAM(N_0,C_0)]	0.01	0.1		N/A[(1)]
[Lck(A, Nsite):ITAM(N_0,C_0)] → Lck(A) + ITAM(N_p,C_0)			0.5	k_{cat} for phosphorylation of N-terminal ITAM is 10-fold greater than k_{cat} for phosphorylation of C-terminal ITAM (61)
Lck(A) + ITAM(N_0,C_0) ↔ [Lck(A, Csite):ITAM(N_0,C_0)]	0.01	0.1		N/A[(1)]
[Lck(A, Csite):ITAM(N_0,C_0)] → Lck(A) + ITAM(N_0,C_p)			0.05	k_{cat} = 0.05 s^{-1} is taken from (92)
ITAM(N_p,C_0) + P ↔ [ITAM(N_p,C_0):P]	0.01	0.1		k_{on} = 0.01 molec^{-1}s^{-1} (0.0062 nM^{-1}s^{-1}) is taken from (93)
				k_{off} = 0.1 s^{-1} is taken from (93)
[ITAM(N_p,C_0):P] → ITAM(N_0,C_0) + P			0.2	k_{cat} = 0.2 s^{-1} is taken from (92, 93)
ITAM(N_0,C_p) + P ↔ [ITAM(N_0,C_p):P]	0.01	0.1		k_{on} = 0.01 molec^{-1}s^{-1} (0.0062 nM^{-1}s^{-1}) is taken from (93)
				k_{off} = 0.1 s^{-1} is taken from (93)
[ITAM(N_0,C_p):P] → ITAM(N_0,C_0) + P			0.2	k_{cat} = 0.2 s^{-1} is taken from (92, 93)
Lck(A) + ITAM(N_p,C_0) ↔ [Lck(A):ITAM(N_p,C_0)]	0.01	0.1		N/A[(1)]
[Lck(A):ITAM(N_p,C_0)] → Lck(A) + ITAM(N_p,C_p)			0.05 used in "ITAM & Lck" model;	k_{cat} = 0.05 s^{-1} is taken from (92)
			0.5 used in "ITAMs" model	k_{cat} = 0.5 s^{-1} is estimated from sensitivity analysis (shown in Fig. S8B)
Lck(A) + ITAM(N_0,C_p) ↔ [Lck(A):ITAM(N_0,C_p)]	0.01	0.1		N/A[(1)]
[Lck(A):ITAM(N_0,C_p)] → Lck(A) + ITAM(N_p,C_p)			0.05	k_{cat} = 0.05 s^{-1} is taken from (92)
ITAM(N_p,C_p) + P ↔ [ITAM(N_p,C_p):P(Nsite)]	0.01	0.1		k_{on} = 0.01 molec^{-1}s^{-1}

				($0.0062\ nM^{-1}s^{-1}$) is taken from (93) $k_{off} = 0.1\ s^{-1}$ is taken from (93)
$[ITAM(N_p,C_p):P(Nsite)] \rightarrow ITAM(N_0,C_p) + P$			0.2	$k_{cat} = 0.2\ s^{-1}$ is taken from (92, 93)
$ITAM(N_p,C_p) + P \leftrightarrow [ITAM(N_p,C_p):P(Csite)]$	0.01	0.1		$k_{on} = 0.01\ molec^{-1}s^{-1}$ ($0.0062\ nM^{-1}s^{-1}$) is taken from (93) $k_{off} = 0.1\ s^{-1}$ is taken from (93)
$[ITAM(N_p,C_p):P(Csite)] \rightarrow ITAM(N_p,C_0) + P$			0.2	$k_{cat} = 0.2\ s^{-1}$ is taken from (92, 93)
$Lck(A) + ITAM(N_p,C_0)] \leftrightarrow [Lck(A, SH2):ITAM(N_p,C_0)]$	0.05 used in "ITAM & Lck" model; 0.00003 used in "ITAMs" model	0.1		$K_D^{exp} = 18.6\ \mu M$ (66) We used $K_D = 5$ nM in "ITAM & Lck" model, which was estimated from sensitivity analysis (shown in Fig. S7A top panel). $K_D^{exp} = 18.6\ \mu M$ (66) We used $K_D = 5\ \mu M$ in "ITAMs" model.
$[Lck(A,SH2):ITAM(N_p,C_0)] \leftrightarrow [Lck(A,SH2):ITAM(N_p,C_0):Csite]$ $[Lck(A,SH2): ITAM(N_p,C_0):Csite] \rightarrow Lck(A) + ITAM(N_p,C_p)$	1.0	0.1	1.0	N/A[1] N/A[1] We have estimated these parameters from sensitivity analysis (shown in Fig. S7B top panel), based on the fact that once Lck-SH2 binds to singly phosphorylated ITAMs, Lck effective concentration increases, and thus promotes the phosphorylation of the neighboring site of ITAMs (similarly to B cells (89)).
$Lck(A) + ITAM(N_0,C_p)] \leftrightarrow [Lck(A, SH2):ITAM(N_0,C_p)]$	0.05 used in "ITAM & Lck" model; 0.00003 used in "ITAMs"	0.1		$K_D^{exp} = 4.7\ \mu M$ (66) We used $K_D = 5$ nM in "ITAM & Lck" model, which was estimated from sensitivity analysis (the same estimate as for N-terminal ITAMs, shown in Fig. S7A top panel). $K_D^{exp} = 4.7\ \mu M$ (66)

	model			
[Lck(A,SH2):ITAM(N_0,C_p)] ↔ [Lck(A,SH2):ITAM(N_0,C_p):Nsite]	1.0	0.1		N/A[1]
[Lck(A,SH2): ITAM(N_0,C_p):Nsite] → Lck(A) + ITAM(N_p,C_p)			1.0	N/A[1] We have estimated these parameters from sensitivity analysis (the same estimate as for N-terminal ITAMs, shown in Fig. S7B top panel), based on the fact that once Lck-SH2 binds to singly phosphorylated ITAMs, Lck effective concentration increases, and thus promotes the phosphorylation of the neighboring site of ITAMs (similarly to B cells (89)).
ITAM(N_p,C_0) + Z ↔ [ITAM(N_p,C_0):Z]	0.00003	0.1		K_D^{exp} = 58.8 µM (66) We used K_D = 5 µM.
ITAM(N_0,C_p) + Z ↔ [ITAM(N_0,C_p):Z]	0.00003	0.1		K_D^{exp} = 44.5 µM (66) We used K_D = 5 µM.
ITAM(N_p,C_p) + Z ↔ [ITAM(N_p,C_p):Z]	0.03	0.1		K_D^{exp} = 3.5-76.6 nM (65, 66) We used K_D = 5 nM.
[ITAM(N_p,C_p):Z] + Lck(A) ↔ [ITAM(N_p,C_p):Z:Lck(A)]	0.05	0.1		N/A[1]
[ITAM(N_p,C_p):Z:Lck(A)] → [ITAM(N_p,C_p):Z(B)] + Lck(A)			0.1	The activity of ZAP-70 WT is greater than the activity of ZAP-70 Y493F mutant (49), thus we used k_{cat} (ZAP-70 basal) = 0.1 s^{-1} that is 4-fold lower than for active ZAP-70.
[ITAM(N_p,C_p):Z(B)] + P_z ↔ [ITAM(N_p,C_p):Z(B):P_z]	0.01	0.1		N/A[1]
[ITAM(N_p,C_p):Z(B):P_z] → [ITAM(N_p,C_p):Z] + P_z			0.2	k_{cat}^{exp} = 0.27 s^{-1} estimated from k_{cat}^{exp}(Dephos Syk) = 0.8 s^{-1} (94)
[ITAM(N_p,C_p):Z(B)] + Lck(A) ↔ [ITAM(N_p,C_p):Z(B):Lck(A, SH2)]	0.05	0.1		N/A[1]
[ITAM(N_p,C_p):Z(B):Lck(A, SH2)] → [ITAM(N_p,C_p):Z(A)] + Lck(A)			0.4	k_{cat}^{exp}(Syk) = 0.5-0.9 s^{-1} (93, 94); k_{cat}^{exp}(ZAP-70) is 3-fold lower than k_{cat}^{exp}(Syk) (94), resulting in k_{cat}(ZAP-70) = 0.3 s^{-1}
[ITAM(N_p,C_p):Z(A)] + P_z ↔ [ITAM(N_p,C_p):Z(A):P_z]	0.01	0.1		N/A[1]
[ITAM(N_p,C_p):Z(A):P_z] → [ITAM(N_p,C_p):Z(B)] + P_z			0.2	k_{cat}^{exp} = 0.27 s^{-1} estimated from

				k_{cat}^{exp}(Dephos Syk) = 0.8 s^{-1} (94)
Lck(A) + [ITAM(N_p,C_p):Z(A)] ↔ [Lck(A):ITAM(N_p,C_p):Z(A)] [Lck(A):ITAM(N_p,C_p):Z(A)] → Lck(I) + [ITAM(N_p,C_p):Z(A)]	0.0025	0.1	0.02 used in "ITAM & Lck" model; 0.05 used in "ITAMs" model	N/A(1) N/A(1) We have estimated these parameters from sensitivity analysis (shown in Fig. S7C and Fig. S7D top panels), based on the fact that tyrosine Y192 site of Lck is a negative regulatory site observed in the current ZAP-70AS+Inhibitor / ZAP-70AS SILAC experiments (shown in Table 1 of main text).
Lck(A) + [ITAM(N_p,C_p):Z(B) ↔ [Lck(A):ITAM(N_p,C_p):Z(B)] [Lck(A):ITAM(N_p,C_p):Z(B)] → Lck(I) + [ITAM(N_p,C_p):Z(B)]	0.0025	0.1	0.02 used in "ITAM & Lck" model; 0.05 used in "ITAMs" model	N/A(1) N/A(1) We have estimated these parameters from sensitivity analysis (the same estimates as for ZAP-70(A), shown in Fig. S7C and Fig. S7D top panels), based on the fact that tyrosine Y192 site of Lck is a negative regulatory site observed in the current ZAP-70AS+Inhibitor / ZAP-70AS SILAC experiments (shown in Table 1 of main text).
Lck(I) + P_{Lck} ↔ [Lck(I):P_{Lck}]	0.015 used in "ITAM & Lck" model; 0.0015 used in "ITAMs" model	0.1		N/A(1) N/A(1)
[Lck(I):P_{Lck}] → Lck(A) + P_{Lck}			0.001 used in "ITAM & Lck" model; 0.0001	N/A(1)

			used in "ITAMs" model;	

(1)Not available. We have estimated these numbers by performing sensitivity analysis of initially guessed kinetic parameters used in calculations.

Table S7. Reactions and kinetic parameters used in calculations for the ZAP-70 allosteric function model. Active Lck is denoted by Lck(A). ITAM(N_0,C_0), ITAM(N_p,C_0), ITAM(N_0,C_p), and ITAM(N_p,C_p) molecules denote unphosphorylated ITAMs, the singly phosphorylated N-terminal tyrosine of ITAMs, the singly phosphorylated C-terminal tyrosine of ITAMs, and doubly phosphorylated ITAM tyrosines, respectively. ZAP-70 molecules exist in three states: inactive ZAP-70, basal ZAP-70, and fully active ZAP-70, which are labeled as Z, Z(B), and Z(A), respectively.

Reactions	**k_{on}, molec^{-1} s^{-1}**	**k_{off}, s^{-1}**	**k_{cat}, s^{-1}**	**Reference**
Lck(A) + ITAM(N_0,C_0) ↔ [Lck(A, Nsite):ITAM(N_0,C_0)]	0.01	0.1		N/A[1]
[Lck(A, Nsite):ITAM(N_0,C_0)] → Lck(A) + ITAM(N_p,C_0)			0.05	k_{cat} = 0.05 s^{-1} is taken from (92)
Lck(A) + ITAM(N_0,C_0) ↔ [Lck(A, Csite):ITAM(N_0,C_0)]	0.01	0.1		N/A[1]
[Lck(A, Csite):ITAM(N_0,C_0)] → Lck(A) + ITAM(N_0,C_p)			0.05	k_{cat} = 0.05 s^{-1} is taken from (92)
ITAM(N_p,C_0) + P ↔ [ITAM(N_p,C_0):P]	0.01	0.1		k_{on} = 0.01 molec^{-1}s^{-1} (0.0062 nM^{-1}s^{-1}) is taken from (93)
				k_{off} = 0.1 s^{-1} is taken from (93)
[ITAM(N_p,C_0):P] → ITAM(N_0,C_0) + P			0.2	k_{cat} = 0.2 s^{-1} is taken from (92, 93)
ITAM(N_0,C_p) + P ↔ [ITAM(N_0,C_p):P]	0.01	0.1		k_{on} = 0.01 molec^{-1}s^{-1} (0.0062 nM^{-1}s^{-1}) is taken from (93)
				k_{off} = 0.1 s^{-1} is taken from (93)
[ITAM(N_0,C_p):P] → ITAM(N_0,C_0) + P			0.2	k_{cat} = 0.2 s^{-1} is taken from (92, 93)
Lck(A) + ITAM(N_p,C_0) ↔ [Lck(A):ITAM(N_p,C_0)]	0.01	0.1		N/A[1]
[Lck(A):ITAM(N_p,C_0)] → Lck(A) + ITAM(N_p,C_p)			0.05	k_{cat} = 0.05 s^{-1} is taken from (92)
Lck(A) + ITAM(N_0,C_p) ↔ [Lck(A):ITAM(N_0,C_p)]	0.01	0.1		N/A[1]
[Lck(A):ITAM(N_0,C_p)] → Lck(A) + ITAM(N_p,C_p)			0.05	k_{cat} = 0.05 s^{-1} is taken from (92)
ITAM(N_p,C_p) + P ↔ [ITAM(N_p,C_p):P(Nsite)]	0.01	0.1		k_{on} = 0.01 molec^{-1}s^{-1} (0.0062 nM^{-1}s^{-1}) is taken from (93)
				k_{off} = 0.1 s^{-1} is taken from (93)
[ITAM(N_p,C_p):P(Nsite)] → ITAM(N_0,C_p) + P			0.2	k_{cat} = 0.2 s^{-1} is taken from (92, 93)
ITAM(N_p,C_p) + P ↔ [ITAM(N_p,C_p):P(Csite)]	0.01	0.1		k_{on} = 0.01 molec^{-1}s^{-1} (0.0062 nM^{-1}s^{-1}) is taken from (93)
				k_{off} = 0.1 s^{-1} is taken from (93)
[ITAM(N_p,C_p):P(Csite)] → ITAM(N_p,C_0) + P			0.2	k_{cat} = 0.2 s^{-1} is taken from (92, 93)

$ITAM(N_p,C_0) + Z \leftrightarrow [ITAM(N_p,C_0):Z]$	0.00003	0.1		K_D^{exp} = 58.8 μM (66) We used K_D = 5 μM.
$ITAM(N_0,C_p) + Z \leftrightarrow [ITAM(N_0,C_p):Z]$	0.00003	0.1		K_D^{exp} = 44.5 μM (66) We used K_D = 5 μM.
$ITAM(N_p,C_p) + Z \leftrightarrow [ITAM(N_p,C_p):Z]$	0.00173 used for ZAP-70 reconstituted and ZAP-70^{AS} cells; 0.00217 used for ZAP-70^{AS}+Inhibitor cells	0.1		K_D^{exp} (ZAP-70 Y315F Y319F) = 96.1 nM (65) K_D^{exp} (ZAP-70 WT) = 76.6 nM (65)
$[ITAM(N_p,C_p):Z] + Lck(A) \leftrightarrow [ITAM(N_p,C_p):Z:Lck(A)]$ $[ITAM(N_p,C_p):Z:Lck(A)] \rightarrow [ITAM(N_p,C_p):Z(B)] + Lck(A)$	0.05	0.1	0.1	N/A[1] The activity of ZAP-70 WT is greater than the activity of ZAP-70 Y493F mutant (49), thus we used k_{cat} (ZAP-70 basal) = 0.1 s^{-1} that is 4-fold lower than for active ZAP-70.
$[ITAM(N_p,C_p):Z(B)] + P_z \leftrightarrow [ITAM(N_p,C_p):Z(B):P_z]$ $[ITAM(N_p,C_p):Z(B):P_z] \rightarrow [ITAM(N_p,C_p):Z] + P_z$	0.01	0.1	0.2	N/A[1] k_{cat}^{exp} = 0.27 s^{-1} estimated from k_{cat}^{exp}(Dephos Syk) = 0.8 s^{-1} (94)
$[ITAM(N_p,C_p):Z(B)] \leftrightarrow [ITAM(N_p,C_p):Z(B, open)]$	0.00217	0.1		K_D^{exp} (ZAP-70 WT) = 76.6 nM (65)
$[ITAM(N_p,C_p):Z(B, open)] + Lck(A) \leftrightarrow [ITAM(N_p,C_p):Z(B, open):Lck(A, SH2)]$ $[ITAM(N_p,C_p):Z(B, open):Lck(A, SH2)] \rightarrow [ITAM(N_p,C_p):Z(A)] + Lck(A)$	0.05	0.1	0.4	N/A[1] k_{cat}^{exp}(Syk) = 0.5-0.9 s^{-1} (93, 94); k_{cat}^{exp}(ZAP-70) is 3-fold lower than k_{cat}^{exp}(Syk) (94), resulting in k_{cat}(ZAP-70) = 0.3 s^{-1}
$[ITAM(N_p,C_p):Z(A)] + P_z \leftrightarrow [ITAM(N_p,C_p):Z(A):P_z]$ $[ITAM(N_p,C_p):Z(A):P_z] \rightarrow [ITAM(N_p,C_p):Z(B, open)] + P_z$	0.01	0.1	0.2	N/A[1] k_{cat}^{exp} = 0.27 s^{-1} estimated from k_{cat}^{exp}(Dephos Syk) = 0.8 s^{-1} (94)
$[ITAM(N_p,C_p):Z(B, open)] + P_z \leftrightarrow [ITAM(N_p,C_p):Z(B, open):P_z]$ $[ITAM(N_p,C_p):Z(B, open):P_z] \rightarrow [ITAM(N_p,C_p):Z] + P_z$	0.01	0.1	0.2	N/A[1] k_{cat}^{exp} = 0.27 s^{-1} estimated from k_{cat}^{exp}(Dephos Syk) = 0.8

				s^{-1} (94)

[(1)]Not available. We have estimated these numbers by performing sensitivity analysis of initially guessed kinetic parameters used in calculations.

Table S8. Sensitivity analysis of the concentrations of signaling molecules used in calculations for the "ITAM and Lck" and "ITAMs" models. The variation in the number of molecules for every species was in the following parameter range: 100, 500, 1000, 1500, and 2000 molecules. Lck(A) denotes active Lck; ITAM(N_0,C_0) represents unphosphorylated ITAMs; P represents phosphatases that dephosphorylate singly and doubly phosphorylated ITAMs; Z denotes ZAP-70; P_z represents phosphatases that dephosphorylate basal and active ZAP-70; P_{Lck} represents phosphatases that dephosphorylate inactive Lck.

Species	Valid parameter range (No. of molecules)	Result
Lck(A)	>500	no qualitative change
ITAM(N_0,C_0)	>500	no qualitative change
P	>100	no qualitative change
Z	>100 and <1000 in the "ITAM and Lck" model; all range in the "ITAMs" model	no qualitative change
P_z	>100 and <1000	no qualitative change at high concentration: all ZAP-70 is dephosphorylated and ZAP-70 protective function dominates
P_{Lck}	>100 in the "ITAM and Lck" model; all range in the "ITAMs" model	no qualitative change

Table S9. Sensitivity analysis of the kinetic parameters used in calculations for the "ITAM and Lck" model. The variation in the kinetic parameters for every chemical reaction was in the following parameter range: 0.001, 0.01, 0.1, 0.5, 1.0, 3.0, and 5.0 s^{-1}. Lck molecules exist in two states: active Lck and inactive Lck, which are represented by Lck(A) and Lck(I), respectively. Lck(A, SH2) denotes the noncatalytic SH2 domain of Lck. ITAM(N_0,C_0), ITAM(N_p,C_0), ITAM(N_0,C_p) and ITAM(N_p,C_p) molecules denote unphosphorylated ITAMs, the singly phosphorylated N-terminal tyrosine of ITAMs, the singly phosphorylated C-terminal tyrosine of ITAMs, and doubly phosphorylated ITAM tyrosines, respectively. ZAP-70 molecules exist in three states: inactive ZAP-70, basal ZAP-70, and fully active ZAP-70, which are represented by Z, Z(B), and Z(A), respectively.

Reactions	**Valid parameter range (k_{on} molec^{-1}s^{-1}; k_{off}, k_{cat} s^{-1})**	**Result**
Lck(A) + ITAM(N_0,C_0) ↔ [Lck(A, Nsite):ITAM(N_0,C_0)]	k_{on}: greater than 0.001 k_{off}: less than 1.0	k_{on}: no qualitative change k_{off}: no qualitative change
[Lck(A, Nsite):ITAM(N_0,C_0)] → Lck(A) + ITAM(N_p,C_0)	greater than 0.1	no qualitative change
Lck(A) + ITAM(N_0,C_0) ↔ [Lck(A, Csite):ITAM(N_0,C_0)]	k_{on}: less than 0.1 k_{off}: greater than 0.01	k_{on}: no qualitative change k_{off}: no qualitative change
[Lck(A, Csite):ITAM(N_0,C_0)] → Lck(A) + ITAM(N_0,C_p)	greater than 0.01	no qualitative change
ITAM(N_p,C_0) + P ↔ [ITAM(N_p,C_0):P]	k_{on}: less than 0.1 k_{off}: all range	k_{on}: no qualitative change k_{off}: no qualitative change
[ITAM(N_p,C_0):P] → ITAM(N_0,C_0) + P	less than 0.5	no qualitative change
ITAM(N_0,C_p) + P ↔ [ITAM(N_0,C_p):P]	k_{on}: less than 0.1 k_{off}: all range	k_{on}: no qualitative change k_{off}: no qualitative change
[ITAM(N_0,C_p):P] → ITAM(N_0,C_0) + P	greater than 0.01	no qualitative change
Lck(A) + ITAM(N_p,C_0) ↔ [Lck(A):ITAM(N_p,C_0)]	k_{on}: less than 0.1 k_{off}: greater than 0.01	k_{on}: no qualitative change k_{off}: no qualitative change
[Lck(A):ITAM(N_p,C_0)] → Lck(A) + ITAM(N_p,C_p)	all range	no qualitative change
Lck(A) + ITAM(N_0,C_p) ↔ [Lck(A):ITAM(N_0,C_p)]	k_{on}: all range k_{off}: less than 0.1	k_{on}: no qualitative change k_{off}: no qualitative change
[Lck(A):ITAM(N_0,C_p)] → Lck(A) + ITAM(N_p,C_p)	less than 0.1	no qualitative change
ITAM(N_p,C_p) + P ↔ [ITAM(N_p,C_p):P(Nsite)]	k_{on}: greater than 0.01 k_{off}: less than 0.5	k_{on}: no qualitative change k_{off}: no qualitative change
[ITAM(N_p,C_p):P(Nsite)] → ITAM(N_0,C_p) + P	greater than 0.1 and less than 0.5	no qualitative change
ITAM(N_p,C_p) + P ↔ [ITAM(N_p,C_p):P(Csite)]	k_{on}: less than 0.1 k_{off}: greater than 0.01	k_{on}: no qualitative change k_{off}: no qualitative change
[ITAM(N_p,C_p):P(Csite)] → ITAM(N_p,C_0) + P	greater than 0.1 and less than 0.5	no qualitative change
Lck(A) + ITAM(N_p,C_0)] ↔ [Lck(A, SH2):ITAM(N_p,C_0)]	k_{on}: greater than 0.01 and less than 0.1 k_{off}: less than 1.0	k_{on}: no qualitative change (shown in Fig. S7A top panel) k_{off}: no qualitative change; at high rates the N-terminal ZAP-70 null / ZAP-70 reconstituted SILAC ratio is greater than C-terminal one
[Lck(A,SH2):ITAM(N_p,C_0)] ↔ [Lck(A,SH2):ITAM(N_p,C_0):Csite]	k_{on}: greater than or equals to 0.5	k_{on}: no qualitative change (shown in Fig. S7B top panel)

	k_{off}: less than 1.0	k_{off}: no qualitative change; at high rates the N-terminal ZAP-70 null / ZAP-70 reconstituted SILAC ratio is greater than C-terminal one
[Lck(A,SH2):ITAM(N_p,C_0):Csite] → Lck(A) + ITAM(N_p,C_p)	greater than or equals to 0.5	no qualitative change
Lck(A) + ITAM(N_0,C_p)] ↔ [Lck(A, SH2):ITAM(N_0,C_p)]	k_{on}: less than 0.1 k_{off}: all range	k_{on}: no qualitative change k_{off}: no qualitative change
[Lck(A,SH2):ITAM(N_0,C_p)] ↔ [Lck(A,SH2):ITAM(N_0,C_p):Nsite]	k_{on}: all range k_{off}: all range	k_{on}: no qualitative change k_{off}: no qualitative change
[Lck(A,SH2):ITAM(N_0,C_p):Nsite] → Lck(A) + ITAM(N_p,C_p)	all range	no qualitative change
ITAM(N_p,C_0) + Z ↔ [ITAM(N_p,C_0):Z]	k_{on}: less than 0.01 k_{off}: all range	k_{on}: at high rates - observed artifact: N-terminal ITAMs protected by ZAP-70 from dephosphorylation by phosphatases, causing decreased phosphorylation of C-terminal ITAMs in ZAP-70 reconstituted cells (shown in Fig. S8C) k_{off}: no qualitative change
ITAM(N_0,C_p) + Z ↔ [ITAM(N_0,C_p):Z]	k_{on}: less than 0.01 k_{off}: all range	k_{on}: at high rates - observed artifact: C-terminal ITAMs protected by ZAP-70 from dephosphorylation by phosphatases, causing decreased phosphorylation of N-terminal ITAMs in ZAP-70 reconstituted cells (shown in Fig. S8D) k_{off}: no qualitative change
ITAM(N_p,C_p) + Z ↔ [ITAM(N_p,C_p):Z]	k_{on}: less than 0.1 k_{off}: all range	k_{on}: at high rates ZAP-70 protective function dominates over ZAP-70 negative feedback k_{off}: no qualitative change
[ITAM(N_p,C_p):Z] + Lck(A) ↔ [ITAM(N_p,C_p):Z:Lck(A)]	k_{on}: all range k_{off}: all range	k_{on}: no qualitative change k_{off}: no qualitative change
[ITAM(N_p,C_p):Z:Lck(A)] → [ITAM(N_p,C_p):Z(B)] + Lck(A)	greater than 0.01 and less than 0.1	no qualitative change
[ITAM(N_p,C_p):Z(B)] + P_z ↔ [ITAM(N_p,C_p):Z(B):P_z]	k_{on}: greater than 0.001 and less than 0.1 k_{off}: less than 0.5	k_{on}: no qualitative change k_{off}: no qualitative change; at high rates – opposite trend: N- and C- terminal ITAM phosphorylation of ZAP-70AS cells is greater than in ZAP-70AS+Inhibitor cells, since phosphatases unbind before its subsequent

		dephosphorylation, causing an increased contribution from ZAP-70 basal state in both cell types
$[ITAM(N_p,C_p):Z(B):P_z] \rightarrow [ITAM(N_p,C_p):Z] + P_z$	greater than 0.01	no qualitative change
$[ITAM(N_p,C_p):Z(B)] + Lck(A) \leftrightarrow [ITAM(N_p,C_p):Z(B):Lck(A, SH2)]$	k_{on}: all range k_{off}: all range	k_{on}: no qualitative change k_{off}: no qualitative change
$[ITAM(N_p,C_p):Z(B):Lck(A, SH2)] \rightarrow [ITAM(N_p,C_p):Z(A)] + Lck(A)$	greater than 0.1	no qualitative change
$[ITAM(N_p,C_p):Z(A)] + P_z \leftrightarrow [ITAM(N_p,C_p):Z(A):P_z]$	k_{on}: greater than 0.001 and less than or equals to 0.01 k_{off}: less than 0.5	k_{on}: no qualitative change k_{off}: no qualitative change
$[ITAM(N_p,C_p):Z(A):P_z] \rightarrow [ITAM(N_p,C_p):Z(B)] + P_z$	greater than 0.1	no qualitative change
$Lck(A) + [ITAM(N_p,C_p):Z(A)] \leftrightarrow [Lck(A):ITAM(N_p,C_p):Z(A)]$	k_{on}: greater than or equals to 0.001 and less than 0.01 k_{off}: less than 0.5	k_{on}: there is no qualitative change within this valid parameter range (shown in Fig. S7C top panel) k_{off}: no qualitative change; at high rates ZAP-70 unbinds faster before its subsequent catalysis, making ZAP-70 protective function stronger than ZAP-70 negative feedback regulation
$[Lck(A):ITAM(N_p,C_p):Z(A)] \rightarrow Lck(I) + [ITAM(N_p,C_p):Z(A)]$	greater than 0.01 and less than 0.1	no qualitative change; at high rates ZAP-70 negative feedback dominates (shown in Fig. S7D top panel)
$Lck(A) + [ITAM(N_p,C_p):Z(B) \leftrightarrow [Lck(A):ITAM(N_p,C_p):Z(B)]$	k_{on}: greater than 0.001 and less than 0.1 k_{off}: greater than 0.01	k_{on}: no qualitative change k_{off}: no qualitative change
$[Lck(A):ITAM(N_p,C_p):Z(B)] \rightarrow Lck(I) + [ITAM(N_p,C_p):Z(B)]$	less than 0.1	no qualitative change
$Lck(I) + P_{Lck} \leftrightarrow [Lck(I):P_{Lck}]$	k_{on}: all range k_{off}: all range	k_{on}: no qualitative change k_{off}: no qualitative change
$[Lck(I):P_{Lck}] \rightarrow Lck(A) + P_{Lck}$	less than or equals to 0.001	at high rates the negative feedback is weak and the ZAP-70 protective function dominates

Table S10. Sensitivity analysis of the kinetic parameters used in calculations for the "ITAMs" model. The variation in the kinetic parameters for every chemical reaction was in the following parameter range: 0.001, 0.01, 0.1, 0.5, 1.0, 3.0, and 5.0 s^{-1}. Lck molecules exist in two states: active Lck and inactive Lck, which are represented by Lck(A) and inactive Lck(I), respectively. ITAM(N_0,C_0), ITAM(N_p,C_0), ITAM(N_0,C_p) and ITAM(N_p,C_p) molecules denote unphosphorylated ITAMs, the singly phosphorylated N-terminal tyrosine of ITAMs, the singly phosphorylated C-terminal tyrosine of ITAMs, and doubly phosphorylated ITAM tyrosines, respectively. ZAP-70 molecules exist in three states: inactive ZAP-70, basal ZAP-70, and fully active ZAP-70, which are represented by Z, Z(B), and Z(A), respectively.

Reactions	Valid parameter range (k_{on} $molec^{-1}s^{-1}$; k_{off}, k_{cat} s^{-1})	Result
Lck(A) + ITAM(N_0,C_0) ↔ [Lck(A, Nsite):ITAM(N_0,C_0)]	k_{on}: greater than or equals to 0.01 k_{off}: less than 0.5	k_{on}: no qualitative change k_{off}: no qualitative change
[Lck(A, Nsite):ITAM(N_0,C_0)] → Lck(A) + ITAM(N_p,C_0)	greater than 0.1	at low rates ZAP-70 null / ZAP-70 reconstituted ratio for N-terminal ITAM is lower than ratio for C-terminal ITAM, since k_{cat} for phosphorylation of C-terminal ITAM is higher (shown in Fig. S8A)
Lck(A) + ITAM(N_0,C_0) ↔ [Lck(A, Csite):ITAM(N_0,C_0)]	k_{on}: greater than or equals to 0.01 k_{off}: less than 0.5	k_{on}: no qualitative change k_{off}: no qualitative change
[Lck(A, Csite):ITAM(N_0,C_0)] → Lck(A) + ITAM(N_0,C_p)	greater than 0.01	no qualitative change; at high rates ZAP-70 null / ZAP-70 reconstituted ratio for C-terminal ITAM is greater than ratio for N-terminal ITAM, since k_{cat} for phosphorylation of C-terminal ITAM is higher
ITAM(N_p,C_0) + P ↔ [ITAM(N_p,C_0):P]	k_{on}: less than 0.1 k_{off}: all range	k_{on}: no qualitative change k_{off}: no qualitative change
[ITAM(N_p,C_0):P] → ITAM(N_0,C_0) + P	greater than 0.01	no qualitative change
ITAM(N_0,C_p) + P ↔ [ITAM(N_0,C_p):P]	k_{on}: less than 0.1 k_{off}: all range	k_{on}: no qualitative change k_{off}: no qualitative change
[ITAM(N_0,C_p):P] → ITAM(N_0,C_0) + P	less than 0.5	no qualitative change
Lck(A) + ITAM(N_p,C_0) ↔ [Lck(A):ITAM(N_p,C_0)]	k_{on}: greater than 0.001 k_{off}: less than or equals to 0.5	k_{on}: no qualitative change k_{off}: no qualitative change
[Lck(A):ITAM(N_p,C_0)] → Lck(A) + ITAM(N_p,C_p)	greater than 0.1	at low rates ZAP-70 null / ZAP-70 reconstituted ratio for N-terminal ITAM is greater than ratio for C-terminal ITAM (shown in Fig. S8B)
Lck(A) + ITAM(N_0,C_p) ↔ [Lck(A):ITAM(N_0,C_p)]	k_{on}: greater than	k_{on}: no qualitative change

	0.001 k_{off}: less than 1.0	k_{off}: no qualitative change
[Lck(A):ITAM(N_0,C_p)] → Lck(A) + ITAM(N_p,C_p)	less than 0.5	no qualitative change
ITAM(N_p,C_p) + P ↔ [ITAM(N_p,C_p):P(Nsite)]	k_{on}: less than 0.5 k_{off}: all range	k_{on}: no qualitative change k_{off}: no qualitative change
[ITAM(N_p,C_p):P(Nsite)] → ITAM(N_0,C_p) + P	greater than to 0.1	no qualitative change
ITAM(N_p,C_p) + P ↔ [ITAM(N_p,C_p):P(Csite)]	k_{on}: less than 0.5 k_{off}: all range	k_{on}: no qualitative change k_{off}: no qualitative change
[ITAM(N_p,C_p):P(Csite)] → ITAM(N_p,C_0) + P	less than 0.5	no qualitative change
ITAM(N_p,C_0) + Z ↔ [ITAM(N_p,C_0):Z]	k_{on}: less than 0.01 k_{off}: all range	k_{on}: at high rates - observed artifact: N-terminal ITAMs protected by ZAP-70 from dephosphorylation by phosphatases, causing decreased phosphorylation of C-terminal ITAMs in ZAP-70 reconstituted cells (shown in Fig. S8C) k_{off}: no qualitative change
ITAM(N_0,C_p) + Z ↔ [ITAM(N_0,C_p):Z]	k_{on}: less than 0.01 k_{off}: all range	k_{on}: at high rates - observed artifact: C-terminal ITAMs protected by ZAP-70 from dephosphorylation by phosphatases, causing decreased phosphorylation of N-terminal ITAMs in ZAP-70 reconstituted cells (shown in Fig. S8D) k_{off}: no qualitative change
ITAM(N_p,C_p) + Z ↔ [ITAM(N_p,C_p):Z]	k_{on}: less than 0.5 k_{off}: greater than 0.01	k_{on}: at high rates ZAP-70 protective function dominates over ZAP-70 negative feedback k_{off}: no qualitative change
[ITAM(N_p,C_p):Z] + Lck(A) ↔ [ITAM(N_p,C_p):Z:Lck(A)]	k_{on}: less than 0.1 k_{off}: all range	k_{on}: no qualitative change; at high rates – ZAP-70 protective function dominates k_{off}: no qualitative change
[ITAM(N_p,C_p):Z:Lck(A)] → [ITAM(N_p,C_p):Z(B)] + Lck(A)	greater than 0.01 and less than 0.1	no qualitative change
[ITAM(N_p,C_p):Z(B)] + P_z ↔ [ITAM(N_p,C_p):Z(B):P_z]	k_{on}: greater than or equals to 0.01 and less than 0.1 k_{off}: less than 0.5	k_{on}: no qualitative change k_{off}: no qualitative change
[ITAM(N_p,C_p):Z(B):P_z] → [ITAM(N_p,C_p):Z] + P_z	greater than 0.01	no qualitative change
[ITAM(N_p,C_p):Z(B)] + Lck(A) ↔ [ITAM(N_p,C_p):Z(B):Lck(A, SH2)]	k_{on}: greater than 0.001 and less than 1.0 k_{off}: less than 3.0	k_{on}: no qualitative change k_{off}: no qualitative change
[ITAM(N_p,C_p):Z(B):Lck(A, SH2)] → [ITAM(N_p,C_p):Z(A)] + Lck(A)	greater than 0.1	no qualitative change
[ITAM(N_p,C_p):Z(A)] + P_z ↔ [ITAM(N_p,C_p):Z(A):P_z]	k_{on}: greater than 0.001 and less than	k_{on}: no qualitative change

	or equals to 0.01 k_{off}: less than or equals to 0.5	k_{off}: no qualitative change
$[ITAM(N_p,C_p):Z(A):P_z] \rightarrow [ITAM(N_p,C_p):Z(B)] + P_z$	greater than or equals to 0.1	no qualitative change
$Lck(A) + [ITAM(N_p,C_p):Z(A)] \leftrightarrow$ $[Lck(A):ITAM(N_p,C_p):Z(A)]$	k_{on}: greater than or equals to 0.001 and less than 0.01 k_{off}: less than 0.5	k_{on}: no qualitative change k_{off}: no qualitative change
$[Lck(A):ITAM(N_p,C_p):Z(A)] \rightarrow$ $Lck(I) + [ITAM(N_p,C_p):Z(A)]$	greater than 0.01	no qualitative change
$Lck(A) + [ITAM(N_p,C_p):Z(B) \leftrightarrow$ $[Lck(A):ITAM(N_p,C_p):Z(B)]$	k_{on}: greater than 0.001 and less than 0.1 k_{off}: greater than 0.01	k_{on}: no qualitative change k_{off}: no qualitative change
$[Lck(A):ITAM(N_p,C_p):Z(B)] \rightarrow$ $Lck(I) + [ITAM(N_p,C_p):Z(B)]$	greater than 0.01 and less than 0.5	no qualitative change
$Lck(I) + P_{Lck} \leftrightarrow [Lck(I):P_{Lck}]$	k_{on}: all range k_{off}: all range	k_{on}: no qualitative change k_{off}: no qualitative change
$[Lck(I):P_{Lck}] \rightarrow Lck(A) + P_{Lck}$	less than 0.001	at high rates the negative feedback is weak and the ZAP-70 protective function dominates

Table S11. Sensitivity analysis of the concentrations of signaling molecules used in calculations for the ZAP-70 allosteric model. The variation in the number of molecules for every species was in the following parameter range: 100, 500, 1000, 1500, and 2000 molecules. Lck(A) denotes active Lck; ITAM(N_0,C_0) represents unphosphorylated ITAMs; P represents phosphatases that dephosphorylate singly and doubly phosphorylated ITAMs; Z denotes ZAP-70; P_z represents phosphatases that dephosphorylate basal and active ZAP-70.

Species	Valid parameter range (No. of molecules)	Result
Lck(A)	all range	no qualitative change
ITAM(N_0,C_0)	all range	no qualitative change
P	all range	no qualitative change
Z	all range	no qualitative change
P_z	all range	no qualitative change

Table S12. Sensitivity analysis of the kinetic parameters used in calculations for the ZAP-70 allosteric model. The variation in the kinetic parameters for every chemical reaction was in the following parameter range: 0.001, 0.01, 0.1, 0.5, 1.0, 3.0, and 5.0 s^{-1}. Lck molecules exist in two states: active Lck and inactive Lck, which are represented by Lck(A) and inactive Lck(I), respectively. ITAM(N_0,C_0), ITAM(N_p,C_0), ITAM(N_0,C_p) and ITAM(N_p,C_p) molecules denote unphosphorylated ITAMs, the singly phosphorylated N-terminal tyrosine of ITAMs, the singly phosphorylated C-terminal tyrosine of ITAMs, and doubly phosphorylated ITAM tyrosines, respectively. ZAP-70 molecules exist in three states: inactive ZAP-70, basal ZAP-70, and fully active ZAP-70, which are represented by Z, Z(B), and Z(A), respectively.

Reactions	**Valid parameter range (k_{on} molec^{-1}s^{-1}; k_{off}, k_{cat} s^{-1})**	**Result**
Lck(A) + ITAM(N_0,C_0) ↔ [Lck(A,Nsite):ITAM(N_0,C_0)]	k_{on}: all range k_{off}: all range	k_{on}: no qualitative change k_{off}: no qualitative change; at high rates the C-terminal ZAP-70 null / ZAP-70 reconstituted SILAC ratio is greater than N-terminal one, because Lck(A) unbinds faster from ITAMs prior its subsequent catalysis
[Lck(A,Nsite):ITAM(N_0,C_0)] → Lck(A) + ITAM(N_p,C_0)	all range	no qualitative change; at high rates the N-terminal ZAP-70 null / ZAP-70 reconstituted SILAC ratio is greater than C-terminal one (shown in Fig. S9A)
Lck(A) + ITAM(N_0,C_0) ↔ [Lck(A,Csite):ITAM(N_0,C_0)]	k_{on}: all range k_{off}: all range	k_{on}: no qualitative change k_{off}: no qualitative change; at high rates the N-terminal ZAP-70 null / ZAP-70 reconstituted SILAC ratio is greater than C-terminal one, because Lck(A) unbinds faster from ITAMs prior its subsequent catalysis
[Lck(A,Csite):ITAM(N_0,C_0)] → Lck(A) + ITAM(N_0,C_p)	all range	no qualitative change; at high rates the C-terminal ZAP-70 null / ZAP-70 reconstituted SILAC ratio is greater than N-terminal one (shown in Fig. S9B)
ITAM(N_p,C_0) + P ↔ [ITAM(N_p,C_0):P]	k_{on}: all range k_{off}: all range	k_{on}: no qualitative change k_{off}: no qualitative change; at high rates the N-terminal ZAP-70 null / ZAP-70 reconstituted SILAC ratio is greater than C-terminal one
[ITAM(N_p,C_0):P] → ITAM(N_0,C_0) + P	all range	no qualitative change; at high rates the C-terminal ZAP-70 null / ZAP-70 reconstituted SILAC ratio is

		greater than N-terminal one (shown in Fig. S9C)
$ITAM(N_0,C_p) + P \leftrightarrow [ITAM(N_0,C_p):P]$	k_{on}: all range k_{off}: all range	k_{on}: no qualitative change k_{off}: no qualitative change; at high rates the C-terminal ZAP-70 null / ZAP-70 reconstituted SILAC ratio is greater than N-terminal one
$[ITAM(N_0,C_p):P] \rightarrow ITAM(N_0,C_0) + P$	all range	no qualitative change; at high rates the N-terminal ZAP-70 null / ZAP-70 reconstituted SILAC ratio is greater than C-terminal one (shown in Fig. S9D)
$Lck(A) + ITAM(N_p,C_0) \leftrightarrow [Lck(A):ITAM(N_p,C_0)]$	k_{on}: all range k_{off}: all range	k_{on}: no qualitative change k_{off}: no qualitative change
$[Lck(A):ITAM(N_p,C_0)] \rightarrow Lck(A) + ITAM(N_p,C_p)$	all range	no qualitative change
$Lck(A) + ITAM(N_0,C_p) \leftrightarrow [Lck(A):ITAM(N_0,C_p)]$	k_{on}: all range k_{off}: all range	k_{on}: no qualitative change k_{off}: no qualitative change
$[Lck(A):ITAM(N_0,C_p)] \rightarrow Lck(A) + ITAM(N_p,C_p)$	all range	no qualitative change
$ITAM(N_p,C_p) + P \leftrightarrow [ITAM(N_p,C_p):P(Nsite)]$	k_{on}: all range k_{off}: all range	k_{on}: no qualitative change k_{off}: no qualitative change
$[ITAM(N_p,C_p):P(Nsite)] \rightarrow ITAM(N_0,C_p) + P$	all range	no qualitative change
$ITAM(N_p,C_p) + P \leftrightarrow [ITAM(N_p,C_p):P(Csite)]$	k_{on}: all range k_{off}: all range	k_{on}: no qualitative change k_{off}: no qualitative change
$[ITAM(N_p,C_p):P(Csite)] \rightarrow ITAM(N_p,C_0) + P$	all range	no qualitative change
$ITAM(N_p,C_0) + Z \leftrightarrow [ITAM(N_p,C_0):Z]$	k_{on}: less than 0.01 k_{off}: all range	k_{on}: at low rates – no qualitative change; at high rates – observed artifact: the ZAP-70 protects the singly phosphorylated N-terminal ITAMs from dephosphorylation by phosphatases, causing the increased production of the phosphorylated C-terminal ITAMs (shown in Fig. S10A) k_{off}: no qualitative change
$ITAM(N_0,C_p) + Z \leftrightarrow [ITAM(N_0,C_p):Z]$	k_{on}: less than 0.01 k_{off}: all range	k_{on}: at low rates – no qualitative change; at high rates – observed artifact: the ZAP-70 protects the singly phosphorylated C-terminal ITAMs from dephosphorylation by phosphatases, causing the increased production of the phosphorylated N-terminal ITAMs (shown in Fig. S10B) k_{off}: no qualitative change
$ITAM(N_p,C_p) + Z \leftrightarrow [ITAM(N_p,C_p):Z]$	k_{on}: all range	k_{on}: no qualitative change; at high rates the ZAP-70 null / ZAP-70 reconstituted SILAC ratio decreases for N- and C- terminals of ITAMs

	k_{off}: all range	due to the ZAP-70 protective function (shown in Fig. S10C) k_{off}: no qualitative change If K_D of ZAP-70^{AS}+Inhibitor cells equals to K_D of ZAP-70^{AS} cells, the experimental data for ZAP-70^{AS}+Inhibitor / ZAP-70^{AS} SILAC ratio are not reproduced (shown in Fig. S10C)
$[ITAM(N_p,C_p):Z] + Lck(A) \leftrightarrow [ITAM(N_p,C_p):Z:Lck(A)]$	k_{on}: all range k_{off}: all range	k_{on}: no qualitative change k_{off}: no qualitative change
$[ITAM(N_p,C_p):Z:Lck(A)] \rightarrow [ITAM(N_p,C_p):Z(B)]+Lck(A)$	all range	no qualitative change
$[ITAM(N_p,C_p):Z(B)] + P_z \leftrightarrow [ITAM(N_p,C_p):Z(B):P_z]$	k_{on}: all range k_{off}: all range	k_{on}: no qualitative change k_{off}: no qualitative change
$[ITAM(N_p,C_p):Z(B):P_z] \rightarrow [ITAM(N_p,C_p):Z] + P_z$	all range	no qualitative change
$[ITAM(N_p,C_p):Z(B)] \leftrightarrow [ITAM(N_p,C_p):Z(B, open)]$	k_{on}: all range k_{off}: all range	k_{on}: no qualitative change k_{off}: no qualitative change
$[ITAM(N_p,C_p):Z(B, open)] + Lck(A) \leftrightarrow$ $[ITAM(N_p,C_p):Z(B, open):Lck(A, SH2)]$	k_{on}: all range k_{off}: all range	k_{on}: no qualitative change k_{off}: no qualitative change
$[ITAM(N_p,C_p):Z(B, open):Lck(A, SH2)] \rightarrow$ $[ITAM(N_p,C_p):Z(A)] + Lck(A)$	all range	no qualitative change
$[ITAM(N_p,C_p):Z(A)] + P_z \leftrightarrow [ITAM(N_p,C_p):Z(A):P_z]$	k_{on}: all range k_{off}: all range	k_{on}: no qualitative change k_{off}: no qualitative change
$[ITAM(N_p,C_p):Z(A):P_z] \rightarrow$ $[ITAM(N_p,C_p):Z(B, open)] + P_z$	all range	no qualitative change
$[ITAM(N_p,C_p):Z(B, open)] + P_z \leftrightarrow$ $[ITAM(N_p,C_p):Z(B, open):P_z]$	k_{on}: all range k_{off}: all range	k_{on}: no qualitative change k_{off}: no qualitative change
$[ITAM(N_p,C_p):Z(B, open):P_z] \rightarrow$ $[ITAM(N_p,C_p):Z] + P_z$	all range	no qualitative change